DYNAMIC BEHAVIOR OF MICROCANTILEVERS SUBJECTED TO FLUID-STRUCTURE INTERACTION USING MODE SUMMATION METHOD

Pranav Ashtaputre

A thesis

In

The Department

Of

Mechanical and Industrial Engineering

Presented in partial fulfillment of the requirements for the
Degree of Master in Applied Sciences (Mechanical Engineering) at
Concordia University
Montreal, Quebec Canada

January 2012

CONCORDIA UNIVERSITY

School of Graduate Studies

This is to certify that the thesis prepared

By: **Pranav J. Ashtaputre**

Entitled: **Dynamic behavior of microcantilevers subjected to fluid-structure interaction using mode-summation method**

and submitted in partial fulfillment of the requirements for the degree of

Master of Applied Science (Mechanical Engineering)

complies with the regulations of the University and meets the accepted standards with respect to

originality and quality.

Signed by the final examining committee:

_____ Chair
Dr. A. Akgunduz
_____ Examiner
Dr. A. Bagchi
_____ Examiner
Dr. J. Dargahi
_____ Co-Supervisor
Dr. R. Bhat
_____ Co-Supervisor
Dr. M. Packirisamy

Approved by   _____

Dr. A.K.W. Ahmed, MASc Program director
Department of Mechanical and Industrial Engineering

Date_____   _____
Dean Robin Drew
Faculty of Engineering and Computer Science

ABSTRACT

Dynamic behavior of microcantilevers subjected to fluid-structure interaction using Mode Summation method

Pranav Ashtaputre

Several Microsystems exhibit interaction of flexible structures such as beams, plates, membranes with fluid. Some of these systems are micropumps, flow sensors and micro valves. It is crucial to consider the effects of fluid parameters such as density, viscosity, velocity and pressure loading while designing these systems. The design of these systems demand a numerical model to understand the dynamic behavior of various elements involved in these systems. Microcantilever is an important structure which exhibits interaction with fluids in various microsystems. The present thesis focuses on the numerical modeling of dynamics of a microcantilever vibrating under the action of fluid loading. Natural frequencies and mode shapes of cantilever are obtained using characteristic orthogonal polynomials in the Rayleigh Ritz method. Numerical model is formed by solving Euler Bernoulli Equation of beam using mode summation method with normal modes of cantilever. The excitation frequency and fluid pressures are obtained from experimental results are explored for modeling and verification purposes. The results are obtained for the tip deflection of the beam. The results are validated with the results obtained in earlier experiments. The deflection amplitudes from the numerical model and those from experiment are found to be in agreement with each other. A parametric study is also presented with different sizes of microcantilever. The effect of different lengths and widths of

microcantilever on the deflection amplitudes is presented. However, the effect of structural deformation due to the changes in fluid pressure is not considered. The model can be further extended to explore the dynamics of microplate used in micropumps with the help of precise fluid pressure data for a particular dynamic system and mode shapes obtained in free vibration analysis. The model provides the first step towards finding a solution to the problems involving fluid loading on microsystems.

Acknowledgment

Table of Contents

List of Figures

List of Tables

List of Symbols

A   Cross sectional area of beam (m^2)

A_1 Tip deflection amplitude of microcantilever corresponding to excitation

                          frequency f_1

A_2 Tip deflection amplitude of microcantilever corresponding to excitation

                          frequency f_2

AFM   Atomic Force Microscope

B_1, B_2, B_3, B_4 Coefficients in the assumed expression of deflection of cantilever

C   Eigen value of undamped mode of cantilever

D   Flexural rigidity of the plate

E   Modulus of elasticity of beam (N/m^2)

f   Frequency of fluctuation of pump

h   Thickness of the membrane of micropump

I   Moment of inertia of beam (m^4)

k   Stiffness of microcantilever

l   Length of microcantilever

M   Added mass per unit area of oscillating plate

P(x, t)   Uniform distributed fluid pressure loading

P_0 Amplitude of fluid pressure loading

$q_i(t)$ Time history of the displacement of the beam

R   Radius of cantilever bending

t   Time(s)

T_0	Period of the signal
W	Deflection of the membrane of micropump
w	Width of microcantilever
X_1	Non-dimensionalized deflection amplitude corresponding to A_1
X_2	Non-dimensionalized deflection amplitude corresponding to A_2
z	Time step used in Runge Kutta solver
ρ_m	Density of the material of membrane of micropump
$\Delta\sigma$	Difference in surface stresses between the two cantilever surfaces
ν	Poisson's ratio of flexible structure
α	Side ratio of rectangular plate
ω	Excitation frequency of force
ζ	Total damping ratio

Chapter 1: Introduction and thesis objective

The advent of Micro-Electro-Mechanical Systems (MEMS) has led to the development of myriad of revolutionary sensors and actuators. Micro-Electro-Mechanical systems involve miniature technologies containing mechanical elements, sensors, actuators and Electronics integrated on a silicon substrate. Some of these MEMS devices include pressure sensors, force sensors, accelerometers, flow sensors etc. Most MEMS sensors are silicon based and are fabricated using either surface or bulk micromachining. Surface micromachining creates free standing movable structures on top of a substrate using a combination of sacrificial layers and structural layers. In bulk micromachining, the mechanical structures are defined using a removal process where bulk material, typically silicon is etched away. MEMS sensors are being used in vibration and shock monitoring on industrial systems and robotics, guidance and navigation in global positioning systems (GPS), seismometers in earthquake prediction, image stabilization in digital cameras, and automobile safety and stability.

Biosensing is one of the largest sectors in MEMS sensing today. A biosensor utilizes biological recognition system to target molecules or macromolecules. It converts biological or biochemical signal into electrical or optical signal. MEMS biosensors have advantages such as low-cost fabrication and fast response times. MEMS biosensors find applications in water and microbial contamination analysis, clinical diagnosis, fermentation analysis and control, industrial gases and control [53]. The deflection of microcantilever caused by interaction can be utilized to detect biomolecules. Figure 1.1 shows some of the MEMS components.
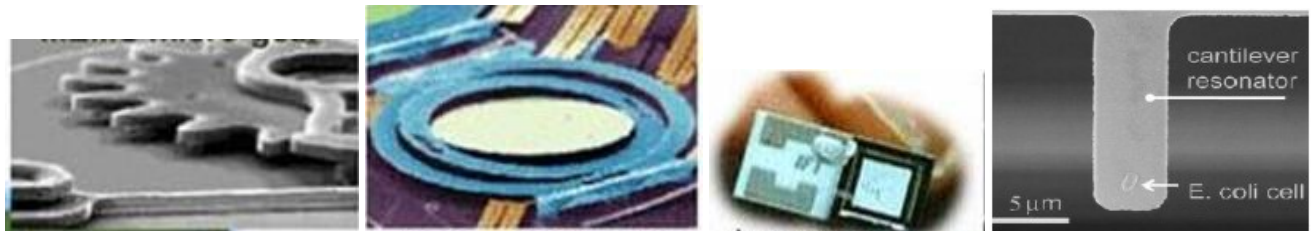
(a)	(b)	(c)	(d)

Figure 1.1: Examples of Microsystems (a) Microgear (b) Micromirror (c) Micropump (d) Microcantilever to detect Bio cell [24].

Most of the sensors and actuators exhibit deformation of flexible structures such as micro beams, micro plates by fluid pressure, electrostatic force or piezoelectric force. The design of these systems involves dynamic analysis of these elements under the action of these forces. The systems involving structural deformation caused by fluid flows are microflow sensors, micro cantilever sensors, micropumps etc. In each of such systems, fluid flow leads to vibration of structure. The dynamic analysis of microstructures is important so as to study the design, implementation, maintenance and repair of these systems. The present work deals with the numerical modeling of MEMS cantilevers. The model can be useful to understand the dynamics of microcantilevers under fluid dynamic loading.

1.1 Micro-Electro Mechanical Systems (MEMS)

The advent of miniature sensing devices has been quite rapid since micro fabrication techniques were developed. Figure 1.2 [42] gives better understanding of the length scales in meter in MEMS. A human hair has a diameter of about 0.1 mm and a nanotube has a diameter of 1 nm.

2
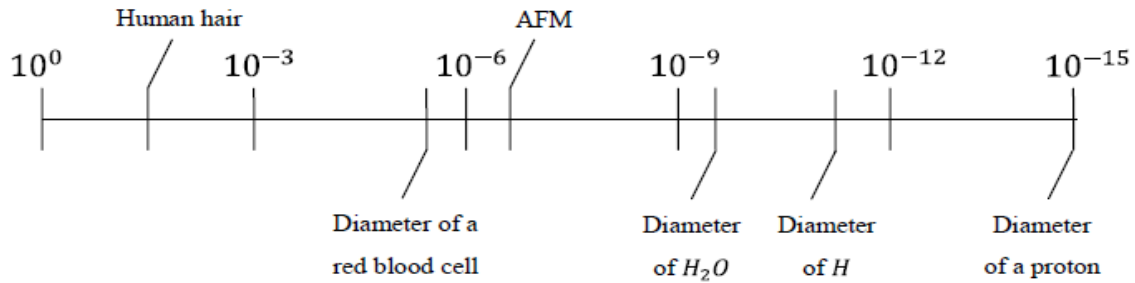
Figure 1.2: Comparison of different length scales (in meter) [42].

Micro cantilevers, micro pumps, micro viscosity sensors, micro flow sensors, micro valves are some of the examples of the micro fluidic devices that involve microfluidic structure interaction. The principle of operation and applications of these devices are discussed in this section. The performance of all of these devices involves fluid-structure interaction that will be studied in this thesis.

1.1.1 Micro Cantilevers

The microcantilever is a widely used component in microsystems. Its flexibility and versatility make it a popular component in a myriad of applications. MEMS cantilevers are used as sensors, transducers, probes, needles, transport mechanisms, resonators, latches, switches and relays. Micro cantilevers find diverse applications in sensing mechanisms [1]. They overcome the drawbacks incurred by conventional sensors since they need extensive packaging. MEMS cantilever sensors can be integrated with whole Electronics on a single chip. The micro-cantilevers can be used in both static as well as dynamic modes [2, 3]. The response of a micro cantilever can be utilized to measure many parameters such as flow rate, fluid pressure, density, viscosity etc. There are several methods employed to detect the deflection of the micro cantilever such as optical deflection, the interferometry deflection, the optical diffraction grating, the charge coupled device, the piezoresistive method etc. Micro cantilever sensors possess high

3

sensitivity, low cost, simple fabrication procedure and quick response. Figure 1.3 [1] explains various sensing applications with the help of micro cantilevers.

SENSING APPLICATIONS OF MICROCANTILEVER

In Medicine & biology
- Lab-on-a-chip
- Blood Glucose monitoring
- Detection of DNA & protein
- Detection of PSA
- Detection of point mutations
- Detection of single Vaccinia particles
- Detection of Myoglobin
- Detection of cells & microorganisms
- Detecting hybridization of DNA
- Detection of Escherichia Coli
- Detection of low-density lipoproteins(LDL's)

In Chemistry & Environmental Monitoring
- Detection of density/viscosity of different liquids
- Detection of humidity
- Detection of temperature & heat changes
- Detection of Infrared & & UV radiations
- Detection of lead & toluene in water
- Detection of nerve agents namely organophosporous compounds
- Detection of ethanol in water
- To detect electrochemical decomposition of polyaniline
- Detection of explosives (nose-on-a-chip)
- To sense mechanical response of living cells
- To count number of bacteria in air
- Detection of change in pH or salt concentration
- Measure analyte vapours in gas phase
- To detect concentration of herbicides
- To detect mercury vapour & mercaptane
- To measure changes in fluid pressure,flow rates and sound wave velocities

Figure 1.3: Sensing applications of microcantilever

The most common properties of a microcantilever used in sensing are its natural frequency and its deflection.
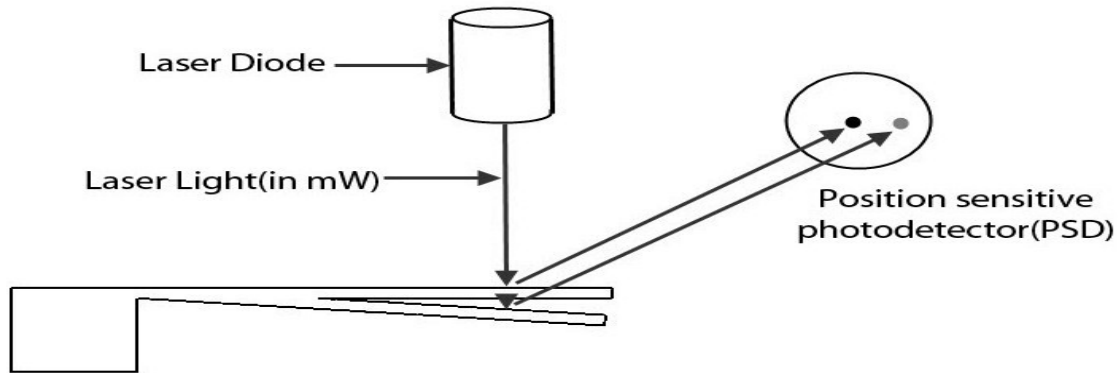
Figure 1.4: Optical method to detect micro cantilever deflection[1]

As shown in the figure, the reflected Laser light from micro cantilever is seen at a different position on the PSD. Depending on the distance between the two positions of the Laser beam on the PSD, the deflection of the micro cantilever is determined.

1.1.2 Types of micro cantilever based sensors

A change in the cantilever deflection or its natural frequency can be employed to measure various parameters of a fluid. A highly viscous medium as well as an added mass [8] will damp the cantilever oscillation and lower its fundamental resonant frequency. Microcantilevers can also be excited using piezoelectric actuators and used as sensors [23].

Micro cantilevers can also be used as humidity sensors when they are coated with Gelatin [25]. Gelatin binds to the water vapors in the atmosphere causing bending of the micro cantilever. Any amount of added mass present on the surface of the cantilever would cause change in its

deflection and natural frequency. Cantilevers coated with hygroscopic materials such as phosporic acid can be used as a sensor for detecting water vapor with pictogram mass resolution [26].

Micro cantilevers with different thermal expansion coefficients can be used to detect changes in temperature [26] due to bimetallic effect. They can be used as micro calorimeters to study the heat evolution in catalytic chemical reactions and enthalpy changes in phase transitions.

Micro cantilevers have been used to detect a concentration of 10^{-9} M $CrO_{4}2$- in a flow cell [27]. In this device, a self-assembled layer of triethyl-12-mercaptododecyl ammonium bromide on the gold-coated microcantilever surface was used. The adsorption of ions causes bending of the beam. Microcantilevers could be used for the chemical detection of a number of gaseous analytes. A multielement sensor array device employing microcantilevers can be made to detect various ions simultaneously.

1.1.3 Modes of operation of micro cantilever

The mode of operation of a cantilever can be divided based upon the measured parameter; structural deformation or resonant frequency. It is called as static mode and dynamic mode, respectively.

Static mode is observed in cantilever based molecular sensors in which static deflection is utilized to measure the amount of material adsorbed onto the microcantilever surface. The difference in adsorption on top and bottom surfaces will cause deflection of the cantilever. Also, it leads to changes in the surface stress. If the difference in surface stresses between the two cantilever surfaces is Δσ and the radius of cantilever bending is R [3], then

$$\frac{1}{R} = \frac{6(1-\upsilon)}{Et^2} \Delta\sigma$$

(1.1)

In dynamic mode, a cantilever is oscillated (by external actuation including piezooscillators), at various excitation frequencies to find out natural frequency. As it is known, the resonant frequency changes with the change in spring constant 'k' and mass of the cantilever 'm'. Unlike the static mode operation, in dynamic mode operation the cantilever can be functionalized on both surfaces. As molecules get adsorbed on the cantilever surface(s) mass or spring constant or both can change [3]. Additionally, adsorption induced surface stresses on the cantilever also changes the frequency of the cantilever. This results in a change in resonant frequency. However, if deflection of only the free end is needed, the motion of an oscillating cantilever can be analogous to lumped spring-mass system which can be described by the second order differential equation.

1.1.4 Micro Valves

Micro cantilever based valves are passive one-way valves where a flap over a duct controls the flow. The applications of these valves are in micropumps, chemical analysis systems and miniaturized chemical reactors. Figure 1.5[50] shows a cantilever based micro valve.
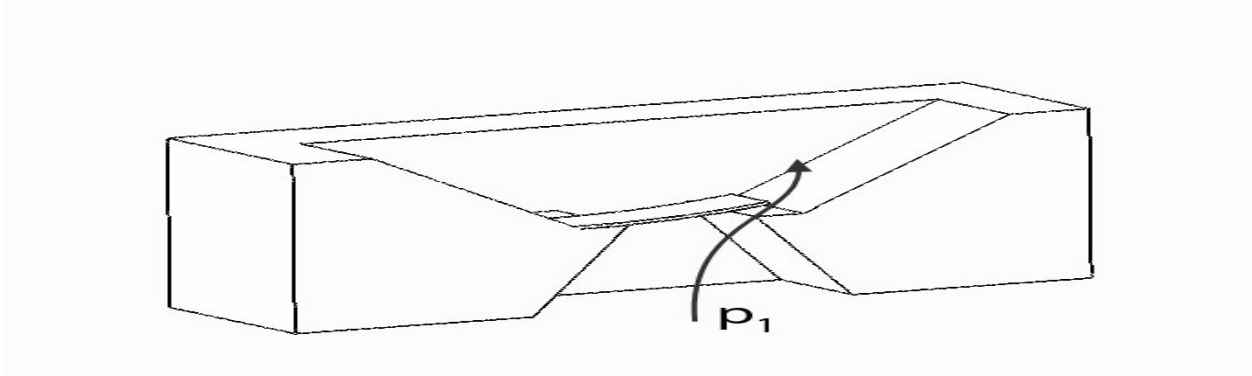
Figure 1.5:Micro cantilever based valve [50]

1.1.5 Micro Pump

Micro pumps are integral part of a micro fluidic system. Following shows a broad classification of micropumps reviewed by D. J. Laser and J. G. Santiago [5]. Micropumps are inherent part of Microfluidics where flow requirement can be in the range of micro or nano litre. The effect of fluid loading on the moving membrane of the pump needs to be considered in the design of these pumps. Classification of micropumps is presented in the following section.

Two main categories of micropumps are displacement and dynamic types.

1. Displacement micropumps are classified as follows.

    i)   Reciprocating: They are classified as diaphragm pumps and piston pumps. Further, diaphragm pumps are divided based on method on actuation such as piezoelectric, thermopneumatic, electrostatic, pneumatic. Based on the type of valves, they are classified as flap valve based or diffuser – nozzle based. Again, depending on the number of chambers, they are categorized as single chamber or multiple chambers.

ii)   Aperiodic: These pumps can be classified as pneumatic or thermal or electrochemical.

2. Dynamic micropumps are classified as follows.

    i)   Centrifugal

    ii)   Electrohydrodynamic which can be injection, induction or conduction type.

    iii)   Magnetohydrodynamic (AC or DC)

Valveless micro pumps have been quite an interesting area of research since they eliminate the disadvantages of complex design with valves. Also, the possibility of fluids trapped while pumping fluids containing particles into these valves is completely eliminated. During the supply mode, the actuator displaces up increasing the total volume of the chamber and thus allowing the intake of fluid into the chamber. During the pump mode, the actuator moves down decreasing the total volume of the chamber and pumping the fluid out.
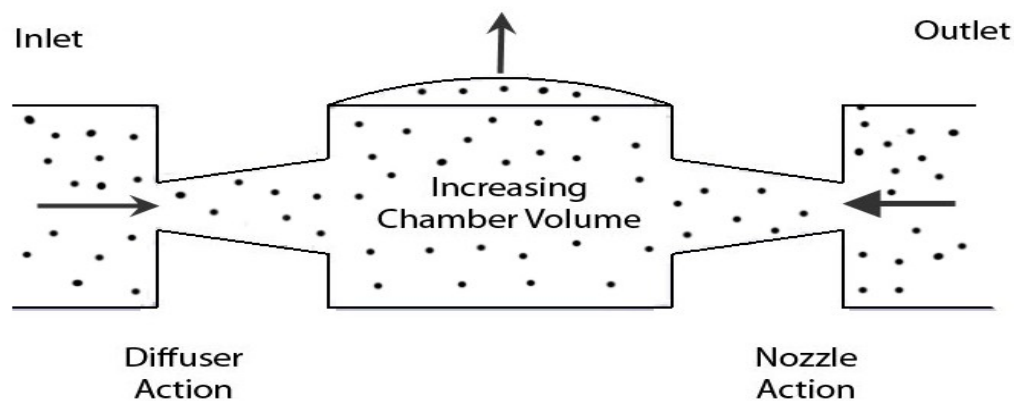
Figure 1.6: Principle of operation during supply mode of valveless micropump[6]
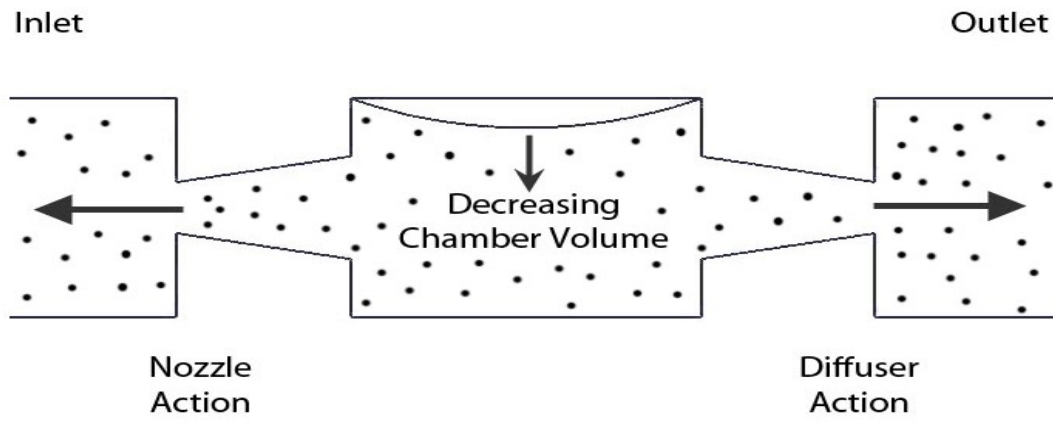
Figure 1.7: Principle of operation during pump mode of valveless micropump[6]

1.1.6 Micro cantilever flow sensors

MEMS based flow sensors are extensively used in flow measurement in the fields such as medical instrumentation, process control and environmental monitoring. As shown in the Figure 1.8 [28] the microcantilevers with piezoresistors on them are employed for flow sensing.
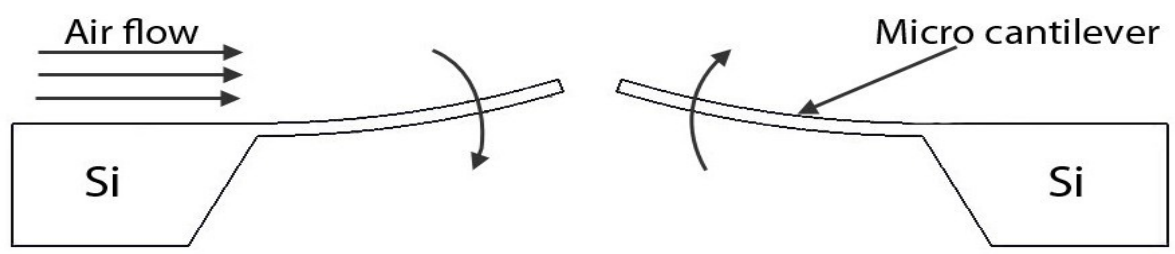
Figure 1.8: Flow sensing with microcantilevers [28]

The beams get deflected due to the fluid flowing on the cantilevers. The deflection of the beams causes change in the cross-sectional area further causing change in the resistance of the piezoresistor. The flow velocity and direction are calculated by measuring this change in the resistance.

1.2   Literature review

The literature is divided into vibration modeling of plates and beams under the action of fluid loading. It is focused on frequency response of micro cantilevers and micro plates oscillated by fluid flows.

1.2.1 Structures subjected to Fluid-Structure Interaction systems (FSI)

The interaction of a flexible structure with a flowing fluid in which it is submerged gives rise to a variety of physical phenomena with applications in many fields of engineering, such as stability and response of aircraft wings, flow of blood through arteries, response of bridges and tall buildings to winds, vibration of turbine and compressor blades, and vibration of cantilevers in fluid. Fluid-structure interaction takes place when fluid flow causes deformation of the structure and deformation of the structure changes boundary conditions of the fluid flow. The cantilever-based FSI systems include Atomic Scope Microscopes, flow sensors, density and viscosity sensors and the frequency response of such systems is an important parameter in order to understand the behavior of such physical systems where both fluid and solid domains have to be modeled. There are many applications where cantilevers are made to vibrate under the action of fluid flow.

Many experimental and numerical analyses of micro cantilever and micro plates vibrating in fluids have been reported in literature. Most of these models report frequency analysis of objects under the action of fluid flows. The interaction can take place due to fluid flow which can be perpendicular or parallel to the neutral axis of a cantilever or a plate.

1.2.2 Fluid-Structure Interaction of a plate

Most of the Micro-Electro-Mechanical Systems have plate as an integral part. As an example, flexible membrane of a micropump is excited by a piezoelectric disk which actuates the fluid flow in the pump chamber. In this case, the interaction between fluid and the membrane clamped at all ends takes place after the membrane is actuated with the help of piezoelectricity. G Song et al [7] performed numerical analysis of piezoelectrically actuated valveless micropump. The simulation model used by them is as follows.

The governing equation of thin clamped membrane used in the simulation is

$$D\nabla^4 W + \rho_m h \frac{\partial^2 W}{\partial t^2} = f - P_d$$

(1.2)

where f is the periodic actuating force exerted by the piezoelectric disk on the pump membrane. P_d is the dynamic pressure exerted by the fluid on the pump membrane. In his model, dynamic pressure has been obtained by solving Navier-Stokes equation, described below at each time step.

$$\rho_l \frac{\partial \vec{v}}{\partial t} = \rho_l g + \mu \nabla^2 \vec{v} - \nabla r$$

(1.3)

$$\frac{\partial \rho_l}{\partial t} + (v.\nabla)\rho_l = 0$$

(1.4)

where ρ_l is the density of the fluid.

μ is the viscosity of the fluid.

$\vec{v}$ is the velocity of the fluid.

In this work, the authors found the deflection of the pump membrane at various actuation frequencies considering the fluid coupling.

The concept of added mass is also one of the ways of expressing fluid-structure interactions when fluid loading causes structural vibration. When a solid structure undergoes fluid loading, the fluid around the microstructure constitute to the inertial force on the structure. When a structure vibrates in a certain fluid, the inertial effect caused by the fluid changes the dynamic behavior of the structure. The fluid surrounding plate creates an added mass effect contributing to the kinetic energy of the fluid.

Yadykin et al. [8] reviewed and presented a numerical analysis of fundamental properties of the added mass of a plane flexible plate oscillating in a fluid. The authors presented following expression to determine added mass per unit area of the oscillating plate.

$$M = -\frac{\int_0^b \int_0^L \Delta P \frac{\partial y}{\partial t} dxdy}{\int_0^b \int_0^L \frac{\partial y}{\partial t} \frac{\partial^2 y}{\partial t^2} dxdy}$$

(1.5)

where ΔP is the fluid pressure loading caused by the deflections of the oscillating plate. y is the deflection of the plate. The authors reviewed various expressions for fluid pressure loadings

leadings to deflections of the plate. $\dfrac{\partial y}{\partial t}$ and $\dfrac{\partial^2 y}{\partial t^2}$ are velocity and acceleration of the oscillating

plate at each time step respectively.

Lucey and Carpenter [13] have obtained fluid loading on the flexible plate as

$$\Delta P(X,Y,t) = \frac{\rho L}{\pi}\left[F_I + UF_D + U^2 F_S\right]$$

(1.6)

where U is the constant velocity of the fluid, t is time.

Y(X, t) and L are surface displacement and length, respectively, of the plate.

The terms F_I, F_D and F_S are called as aerodynamic inertia, damping and stiffness, respectively.

In this work, it was found that the amount of added mass is a function of the mode number.

From the expression of added mass, it can be seen that its value changes at each time step. Also,

it was concluded that the amount of added mass decreases in higher modes of vibration.
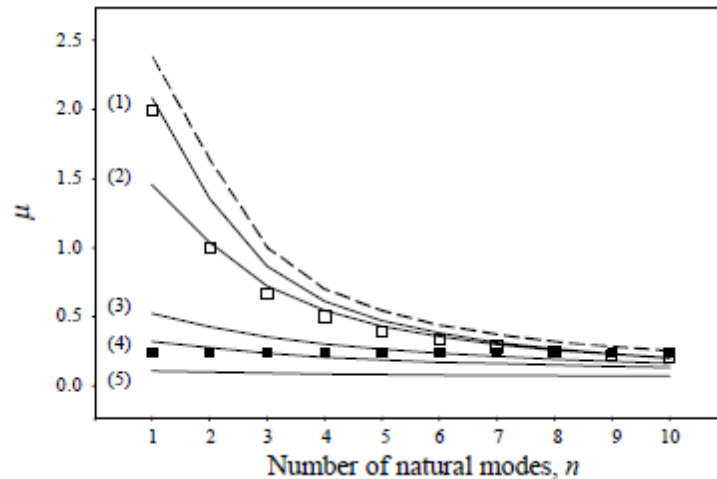
Figure 1.9: The dependance of added mass coefficient on aspect ratio A and numer of natural mode n of the cantilevered plate. 3-D theory:Continuous line (1)A=1.0 (2)A=0.5 (3)A=0.1 (4)A=0.05 (5)A=0.01. 2-D theory:Dotted line;[8]

Also, the authors concluded that the effect of added mass is smaller for plates with low aspect ratios.

Fu and Price [21] studied vibration responses of cantilevered vertical and horizontal square plates partially and fully submerged in fluid. The effect of submerged plate length on the resonant frequencies of plates has been investigated in their work.

Sinha et al. [20] studied vibration characteristics of submerged, perforated plates. In their work, a formula was suggested for the calculation of added mass for perforated plate structures. Also, it was proved that these plates exhibit a decrease in natural frequency when submerged in a fluid. Also, it was concluded that the perforated plates undergo more damping than non-perforated plates.

Pan et al. [30] performed numerical simulation of fluid-structure interaction in a MEMS diaphragm based drop ejector. Ergin and Ugurlu [9] performed linear vibration analysis and found natural frequencies and mode shapes for cantilevered plates partially submerged in fluid.

1.2.3 Fluid-Structure interaction of a Cantilever

Micro cantilevers undergoing fluid-structure interaction can be found in several micro-electro-mechanical systems. G. Rezazadeh et al [10] performed numerical analysis on electrostatically actuated microbeam in an incompressible, inviscid and stationary fluid. He used Lucey and Carpenter's theory [13] to express pressure loading on the cantilever beam in order to find non-dimensional added mass. This added mass has been used into Euler-Bernoulli equation to find the frequency response of the beam under fluid loading as shown in Figure 1.10.
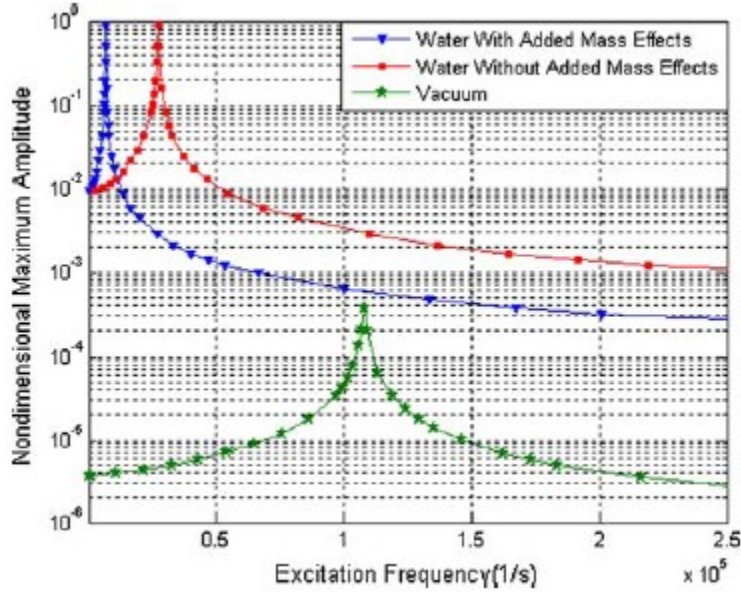
Figure 1.10: Frequency reponse of microbeam with added mass and without added mass by G. Rezazadeh [10]

Sader et al. [51] performed a theoretical analysis of the frequency response of the cantilever beam immersed in a viscous fluid and excited by an arbitrary force. The arbitrary force, in this case has been assumed to be thermal i.e. Brownian motion of the molecules of the surrounding fluid. In this model, the undamped modes of cantilever are considered and deflection of the cantilever is assumed to be a sum of these modes where each mode is excited by the Brownian motion of fluid particles. They presented numerical results of deflection response of AFM cantilevers in his model. The normalized thermal spectra expression presented in Sader's model is as follows.

$$\left(\frac{\partial W(x)}{\partial x}\right)^2 = \frac{3\pi k_B T}{k} \sum_{i=1}^{n} \frac{\alpha_n^2(\omega)}{C_n^4 \int_0^{\infty} \alpha_n^2(\omega)d\omega} \left(\frac{d\phi_n(x)}{dx}\right)^2 \tag{1.7}$$

where W is the deflection function.

$\Phi(x)$ is the undamped mode of a cantilever beam.

k_B is the Bolzmann's constant.

k is the spring constant.

T is the absolute temperature.

$$Z_n(\omega) = \frac{2\sin C_n \tan C_n}{C_n(C_n^4 - B^4(\omega))(\sin C_n + \sinh C_n)} \tag{1.8}$$

$$B(\omega) = C_1 \sqrt{\frac{\omega}{\omega_{vac}}} \left(1 + \frac{\pi \rho b^2}{4\mu} \Gamma(\omega)\right)^{1/4} \tag{1.9}$$

for smaller Reynold number flows,

$$\Gamma(\omega) = \frac{-4i}{\text{Re}\ln(-i\sqrt{i\,\text{Re}})} \tag{1.10}$$

Reynolds number for the flow is expressed as

$$\text{Re} = \frac{\rho\omega b^2}{4\eta} \tag{1.11}$$

ρ and η are density and viscosity of the fluid.

$$T = \frac{\rho b}{\rho_c h} \tag{1.12}$$

b and h are width and thickness of the beam respectively.

ρ_c is the density of the cantilever material.

17

T gives the ratio of the added mass due to apparent fluid forces to the total mass of the beam.

Q is the quality factor defined as follows.

$$Q = \frac{\dfrac{4\mu}{\pi \rho b^2} + \Gamma_r}{\Gamma_i}$$

(1.13)

Figure 1.11 shows the normalized thermal spectra H resulted from the numerical model by Sader [51].
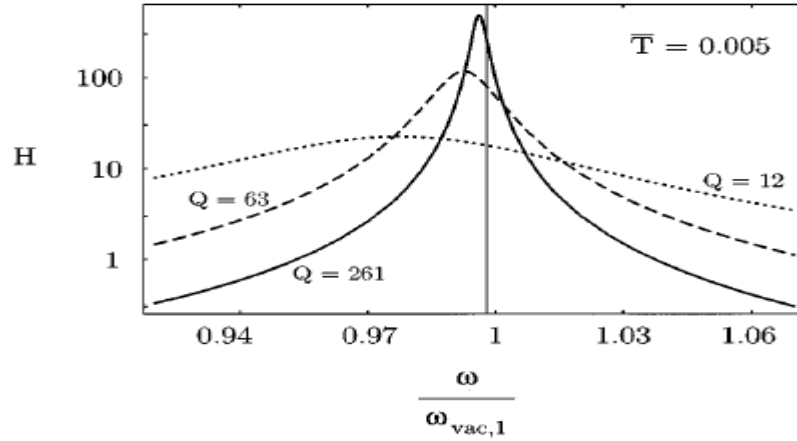
Figure 1.11: Normalized thermal spectra of fundamental mode in Sader's model [51]

Wang et al [16] considered flow-induced vibration of cylinders with large aspect ratios. In his model, the structural part is solved by Euler-Bernoulli theory using normal modes while fluid forces are calculated by finite element method.

Houston et al. [29] determined vibration characteristics of atomic force microscope cantilever operating in liquid. In his work, the behavior of cantilever was simulated simultaneously with the time dependent flow field. The flow field is solved at each time step from the new cantilever velocity.

Similarly, the fluid-structure interaction analysis of micro cantilevers used in Atomic Force microscope operating in viscous fluids has also been performed to study the effect on natural frequency [34-41].

1.3 Thesis Objective, Problem Definition and Overview

1.3.1 Thesis Objective

The main objective of the thesis is to study and model dynamic deflections of microcantilever vibrating under the action of fluid loading. Microcantilevers are being used in several sensing applications in which they are oscillated by fluid flows. The design of these microcantilevers demands a numerical model to predict deflection amplitudes of cantilever under various fluid loading conditions.

1.3.2 Problem Definition

The dynamics of cantilevers vibrating under the action of fluid loading is important in the design of cantilever based sensors. Amplitudes of cantilevers with different excitation frequencies are required to be known so as to design sensors from such cantilevers. In order to determine the amplitudes of micro cantilever, deflection response problem needs to be solved by considering forced vibration under the action of different fluid loading conditions.

1.3.3 Thesis contribution

The dynamics of the cantilever vibrating under fluid loading can be exploited in order to make it applicable in sensing. Various parameters can be studied with the help of numerical analysis of

vibrating cantilevers. The present thesis demonstrates a numerical model to analyze dynamics of micro cantilevers vibrating under the action of fluid force. The numerical analysis of vibration is presented with the help of normal modes of cantilever. The model will be useful to predict performance of microcantilevers with different dimensions vibrating under the action fluid flow.

1.3.4 Overview

The present thesis is organized in six chapters.

Chapter 1: The chapter explains various micro-electro mechanical systems, their applications. It includes literature review on numerical models on fluid-structure interaction. The FSI models are divided into those of beams and plates. Also, it includes thesis contribution, objective and problem definition of the present thesis.

Chapter 2: This chapter includes free vibration analysis of cantilevers using Rayleigh-Ritz method and finding out their natural frequencies. Natural frequencies and mode shapes of Fixed-Free beam are presented.

Chapter 3: This chapter includes free vibration analysis of rectangular plates using Rayleigh-Ritz method. Also, literature review on numerical models on free vibration analysis of plates is included. Natural frequencies and mode shapes of clamped-clamped plate are presented.

Chapter 4: This chapter includes modeling of Euler-Bernoulli equation using Simulink. The mode summation method is explained to solve forced vibration problem using the fluid pressure and excitation frequency determined in earlier experiments. The results are obtained in time domain using Runge Kutta Fourth Order solver in Simulink.

Chapter 5: This chapter includes review of the experimental set up. The model explained in Chapter 4 is applied to the problem in the experiment. The deflection response of micro cantilever is presented in frequency domain. The deflection amplitudes obtained using numerical

model, are compared for six cases with those from experiments. Also, a parametric study is presented with different widths and lengths of microcantilever. The results are plotted for all these sizes at a certain fluid loading. Finally, the deflection amplitudes from these results are non dimensionalized with respect to cantilever properties and fluid loading.

Chapter 6: This chapter presents and conclusion and future work that can be performed with the help of presented model.

Chapter 2: Natural frequency and mode shapes of beams

In order to study the fluid-structure interaction problem, it is essential to study vibrations of flexible structures. Most of the flexible structures are categorized in the following way.

Table 2.1: Flexible structures in dynamic systems

Beams	
Strings	One-Dimensional
Shafts	
Membranes	Two-Dimensional
Plates	
Shell	Three Dimensional

In the present study, cantilever beam and rectangular plate are investigated in order to determine their fundamental frequencies and mode shapes since they are commonly used elements in microstructures. The results of this study will be used in investigating the fluid-microstructure interaction phenomenon.

In the absence of any fluid (i.e. in vacuum), without the action of any external force, analysis of natural frequencies of a beam can be solved by solving Euler-Bernoulli equation. Natural frequencies are required in order to study the response of microstructures when they are excited at its one of their frequencies.

2.1 Euler-Bernoulli Equation of Motion of beam

In the following, Euler-Bernoulli beam is analyzed. Euler-Bernoulli theory does not consider the effects of rotary inertia and shear deformation.

Euler-Bernoulli equation of motion of beam in the absence of an external force is expressed as

$$EI\frac{\partial^4 y(x,t)}{\partial x^4} + \rho A\frac{\partial^2 y(x,t)}{\partial t^2} = 0 \tag{2.1}$$

Let $p = \sqrt{\dfrac{EI}{\rho A}}$

$$p^2\frac{\partial^4 y(x,t)}{\partial x^4} + \frac{\partial^2 y(x,t)}{\partial t^2} = 0 \tag{2.2}$$

We assume that the solution is in the following form.

$$y(x,t) = Y(x)*T(t) \tag{2.3}$$

where Y(x) is a function of shape and T(t) is a function of time.

substituting Equation (2.3) into Equation (2.2), we get after separation of variables,

$$\frac{p^2}{Y(x)}\frac{d^4 Y(x)}{dx^4} = -\frac{1}{T(t)}\frac{d^2 T(t)}{\partial t^2} = \omega^2 \tag{2.4}$$

Equation (2.4) can be written as

$$\frac{d^2 y(x)}{dx^2} - \beta^4 y(x) = 0 \tag{2.5}$$

where $\beta^4 = \rho A\,\omega^2/EI$

Y(x), can be assumed to be in the form.

$$Y(x) = B_1 e^{\beta x} + B_2 e^{-\beta x} + B_3 e^{i\beta x} + B_4 e^{-i\beta x}$$ (2.6)

where B_1, B_2, B_3, B_4 are constants.

Equation (2.6) can also be expressed as

$$Y(x) = C_1 (\cos \beta x + \cosh \beta x) + C_2 (\cos\beta x - \cosh \beta x) + C_3 (\sin\beta x + \sinh \beta x) + C_4 (\sin\beta x - \sinh \beta x)$$ (2.7)

where C_1, C_2, C_3, C_4 are constants in this case.

Natural frequency of the beam is given by

$$\omega = \beta^2 \sqrt{\frac{EI}{\rho A}} = (\beta l)^2 \sqrt{\frac{EI}{\rho A l^4}}$$ (2.8)

2.2 Natural Frequencies and Mode shapes of a Cantilever beam

When a system is given an initial input and then set to vibrate, it is said to be vibrating freely. In this case, the system is said to be vibrating at one or more of its natural frequencies. In the present model, a beam is considered free at one end and fixed at the other end. Table 2.2 shows the boundary conditions of the beam.

Table 2.2: Boundary conditions of cantilever beam.

Fixed End	Deflection Y = 0	Slope dY/dx = 0
Free End	$\dfrac{d^2 Y(L)}{dx^2} = 0$	$\dfrac{d^3 Y(L)}{dx^3} = 0$

Figure 2.1 shows a cantilever beam with its dimensions.
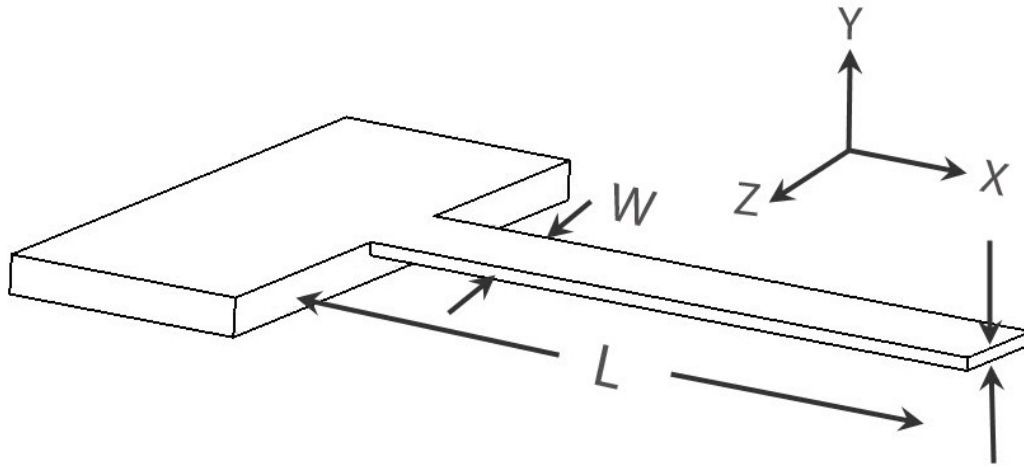
Figure 2.1: Cantilever beam with length L, width w and thickness t. The fixed end is at x=0 and free end is at x=L. The motion is along y-axis.

Applying the first two boundary conditions in Table 2.2 at the fixed end in Equation (2.7)

C1 = C3 = 0

By using the boundary conditions at the free end and solving, we get

$$\cos \beta l \cosh \beta l + 1 = 0 \qquad (2.9)$$

This is the frequency equation of the beam.

The expression for the deflection of the beam becomes

$$Y_n(x) = (\cos \beta_n x - \cosh \beta_n x) - \frac{(\cos \beta_n l + \cosh \beta_n l)(\sin \beta_n x - \sinh \beta_n x)}{(\sin \beta_n l + \sinh \beta_n l)} \qquad (2.10)$$

2.3 Modal analysis of beams

Modal analysis is used to study dynamic response behavior of a structure under vibrational excitation. There are a few numerical methods which can be found in the literature used to perform modal analysis of structures modeled by Euler-Bernoulli beam theory. The Rayleigh-Ritz method is a popular method used to determine natural frequencies and mode shapes of beams and plates due to its simplicity and reasonable accuracy.

Several modal analysis studies can be found in literature. Evensen [22] showed that, for higher modes of vibration, the amplitude-frequency curves of a clamped-clamped beam or a clamped–supported beam tend to approach that of a simply supported beam. The influence of the boundary conditions on the response becomes less pronounced as the mode number increases.

In the present study, free vibration analysis of beam and plate is performed by using boundary characteristic orthogonal polynomials in the Rayleigh-Ritz method. The orthogonal polynomials are obtained by using Gram-Schmidt process described in [11]. The polynomials satisfy geometric boundary conditions of the beam and plate. Results of a square plate are compared with those obtained in [11].

2.3.1 Rayleigh-Ritz method

The deflection of the beam is assumed as the sum of several functions multiplied by constants

$$Y(x) = \sum_{i=1}^{N} a_i \phi_i(x) \qquad (2.11)$$

Φ_i, are functions satisfying the boundary conditions of the beam.

a_i is unknown coefficients.

Maximum kinetic and potential energies of the beam are given by

$$T_{max} = \frac{\rho A \omega^2}{2} \int_0^l \left(\frac{\partial y}{\partial t} \right)^2 dx = \omega^2 T_{max}^* \qquad (2.12)$$

$$U_{max} = \frac{EI}{2} \int_0^l \left(\frac{\partial^2 y}{\partial x^2} \right)^2 dx \qquad (2.13)$$

Equating both the energies,

$$T_{max} = U_{max}$$

Rayleigh quotient is obtained as

$$\omega^2 = \frac{U_{max}}{T_{max}^*}$$

Applying the condition of stationarity of the natural frequencies, with respect to the arbitrary coefficient a_i,

$$\frac{\partial \omega^2}{\partial a_i} = 0$$

This equation yields an eigen value problem as follows.

$$\left([K] - [M] \omega^2 \right) x = 0 \qquad (2.14)$$

where stiffness matrix K and Mass matrix M are given by

$$K = \frac{\partial U_{max}}{\partial a_i} \qquad (2.15)$$

$$M = \frac{\partial T_{max}^*}{\partial a_i} \qquad (2.16)$$

where i = 1, 2, 3 ….. N

27

2.3.2 Generation of boundary characteristic orthogonal polynomials

The boundary characteristic orthogonal polynomials are produced using Gram-Schmidt process described in [11].

The first member (Φ_0) of the set of polynomials is chosen such that it satisfies all boundary conditions of the beam. The rest of the polynomials are constructed in following way.

$$\Phi_1 = (x - B_1)\,\Phi_0 \tag{2.17}$$

$$\Phi_n = (x - B_n)\Phi_{n-1}(x) - C_n\Phi_{n-2}(x) \tag{2.18}$$

$$C_n = \frac{\displaystyle\int_a^b xw(x)\Phi_{n-1}(x)\Phi_{n-2}(x)dx}{\displaystyle\int_a^b w(x)\Phi_{n-2}^2(x)dx} \tag{2.19}$$

$$B_n = \frac{\displaystyle\int_a^b xw(x)\Phi_{n-1}^2(x)dx}{\displaystyle\int_a^b w(x)\Phi_{n-1}^2(x)dx} \tag{2.20}$$

The weight function w (x) is chosen such that

$$\int_a^b w(x)\Phi_n(x)\Phi_l(x)dx = \begin{pmatrix} 0 \ \ if \ \ n \neq l \\ a \ \ if \ \ n = l \end{pmatrix} \tag{2.21}$$

The coefficients of the polynomials are chosen such that the polynomials are orthonormal to each other as follows.

$$\int_0^1 \Phi_n^2(x)dx = 1 \qquad (2.22)$$

2.3.3 Eigen value analysis: Cantilever beam

The first polynomial for a cantilever beam is chosen such that it satisfies all the boundary conditions from Table 2.2. Accordingly, it is obtained as

$$X(x) = 6x^2 - 4x^3 + x^4 \qquad (2.23)$$

The polynomial X(x) is normalized as follows.

$$\Phi_0(x) = \frac{(6x^2 - 4x^3 + x^4)}{\left(\int_0^1 X^2(x)dx\right)^{1/2}} \qquad (2.24)$$

$$\Phi_0(x) = 2.311(6x^2 - 4x^3 + x^4) \qquad (2.25)$$

2.3.4 Results

Further polynomials are produced using Gram-Schimdt process as explained before. These polynomials are used in the Rayleigh-Ritz method and eigen values are obtained for fixed –free beam. Table 2.3 shows first five Eigen values.

Table 2.3: Eigen values of fixed-free beam obtained by Rayleigh-Ritz method

C1	1.87510
C2	4.69409
C3	7.85475
C4	10.99559
C5	14.14005

Figure 2.2-Figure 2.11 show first ten normalized modes plots.
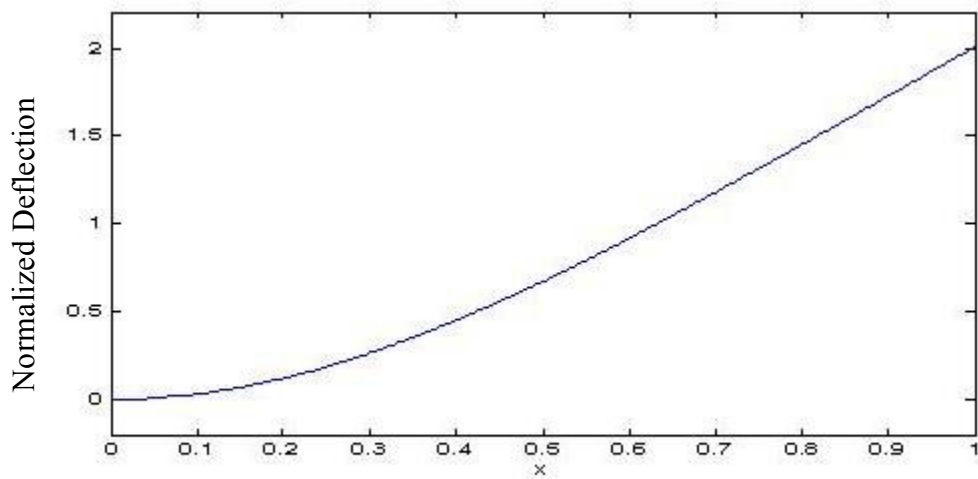
Figure 2.2:Mode 1 of cantilever beam using Rayleigh-Ritz method
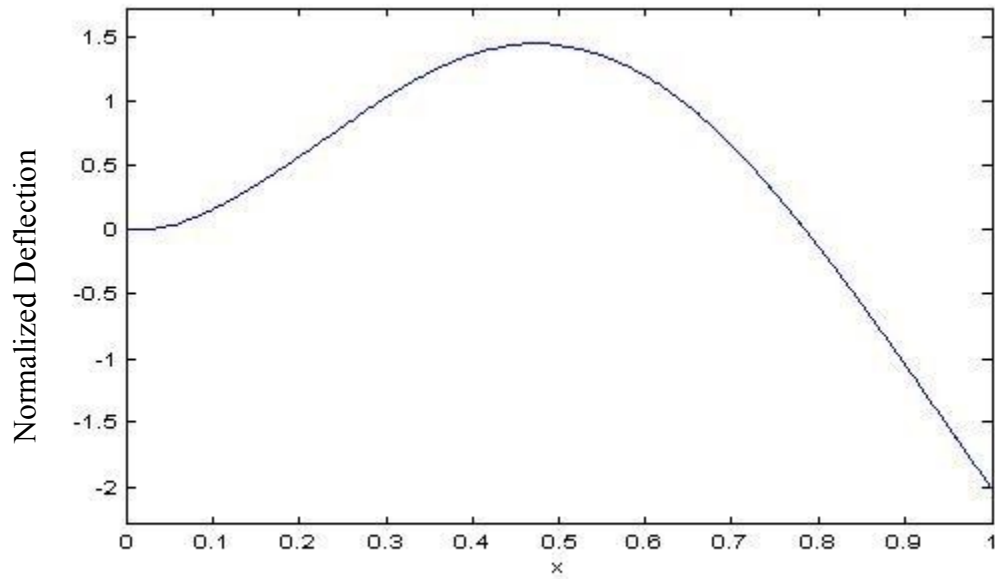
Figure 2.3:Mode 2 of cantilever beam using Rayleigh-Ritz method
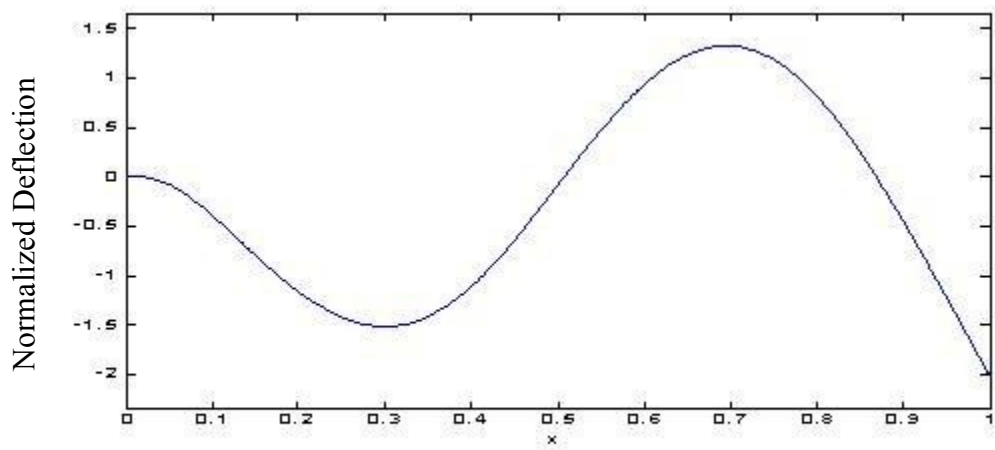
Figure 2.4:Mode 3 of cantilever beam using Rayleigh-Ritz method
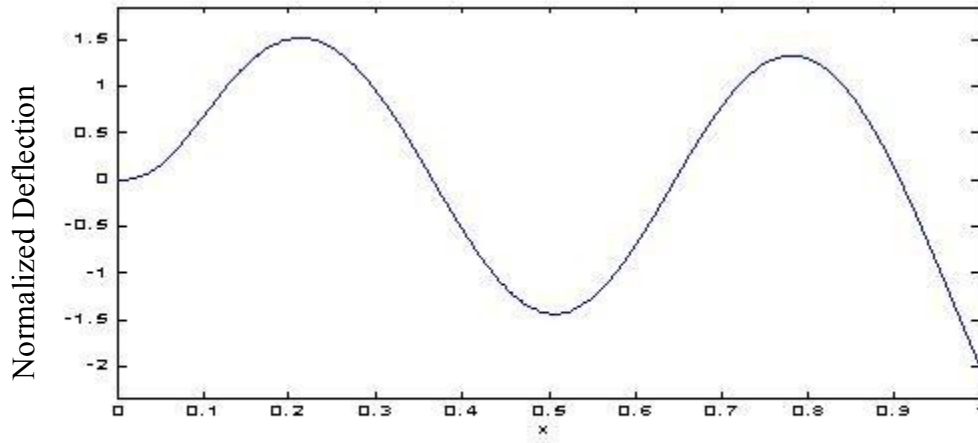
Figure 2.5: Mode 4 of cantilever beam using Rayleigh-Ritz method
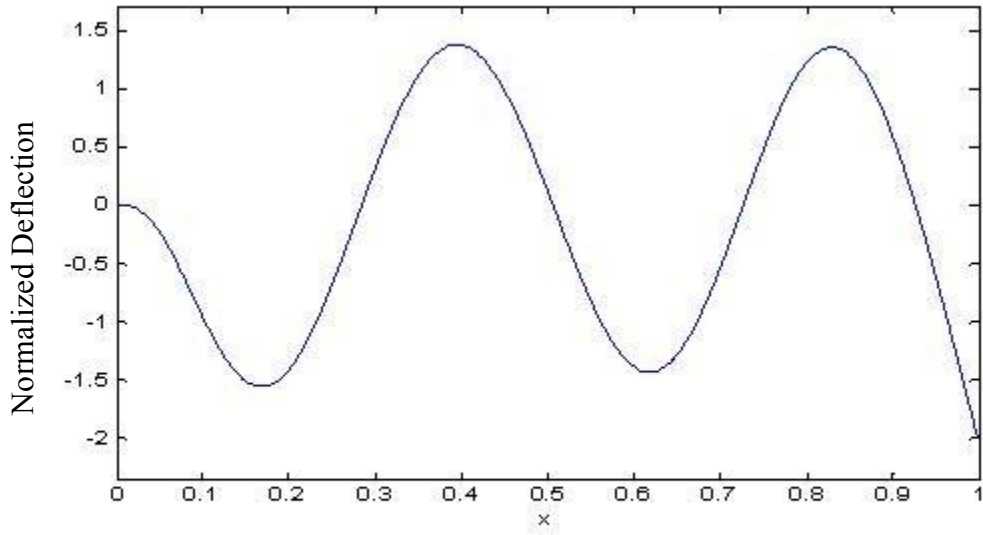
Figure 2.6: Mode 5 of cantilever beam using Rayleigh-Ritz method
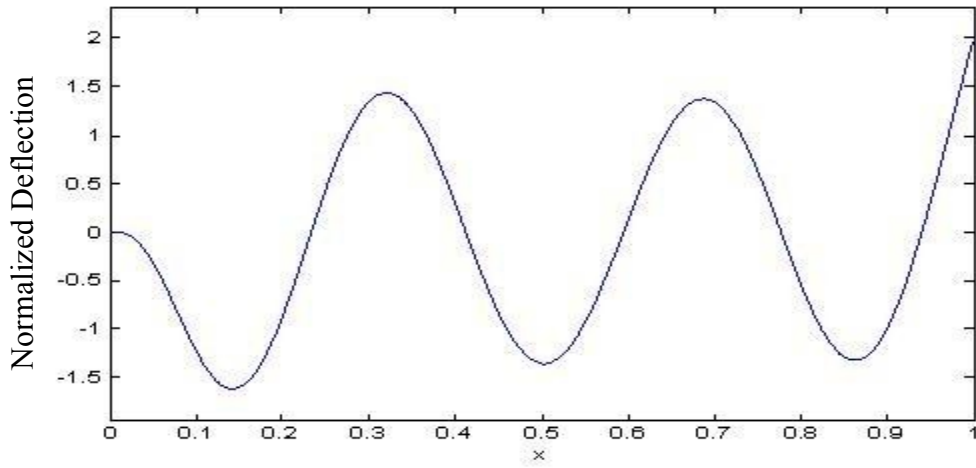
Figure 2.7: Mode 6 of cantilever beam using Rayleigh-Ritz method
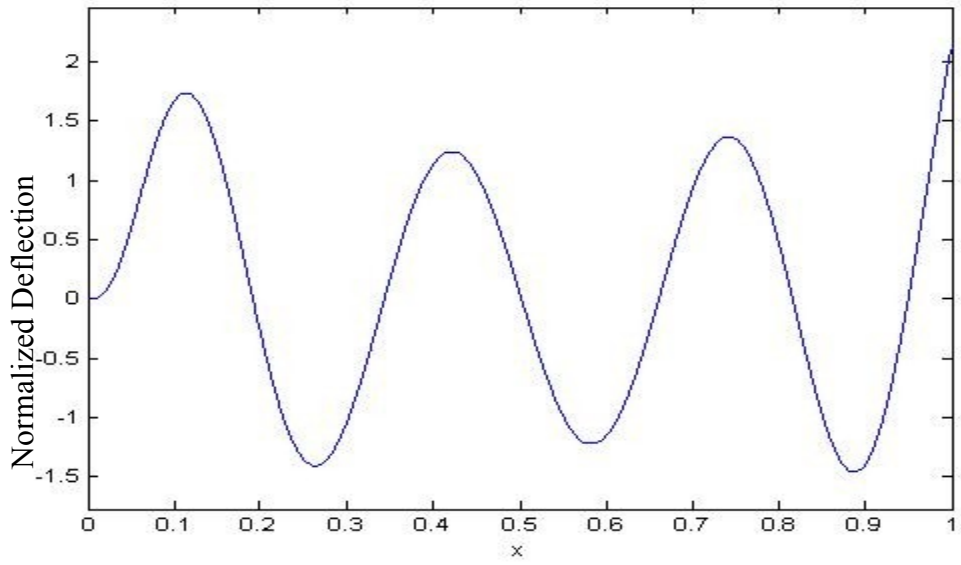
Figure 2.8:Mode 7 of cantilever beam using Rayleigh-Ritz method
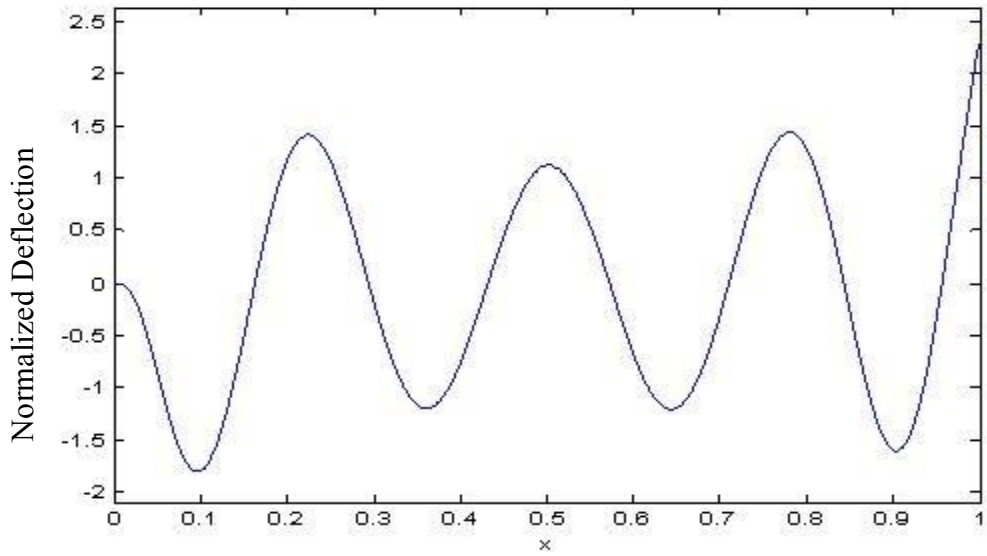
Figure 2.9: Mode 8 of cantilever beam using Rayleigh-Ritz method
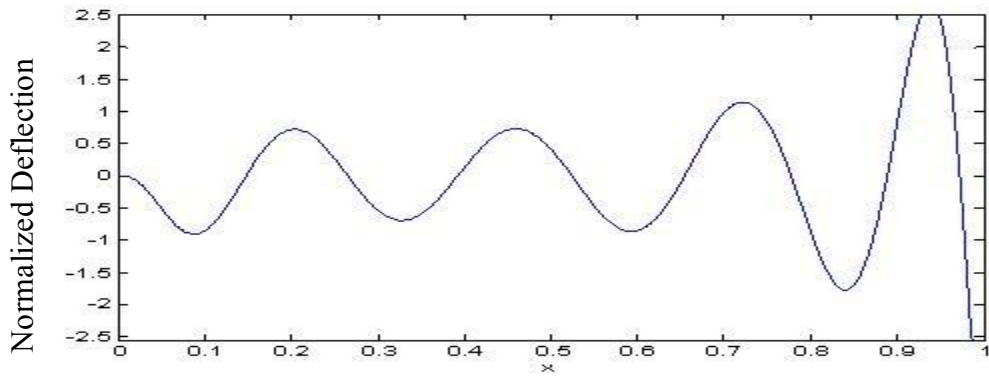
Figure 2.10: Mode 9 of cantilever beam using Rayleigh-Ritz method
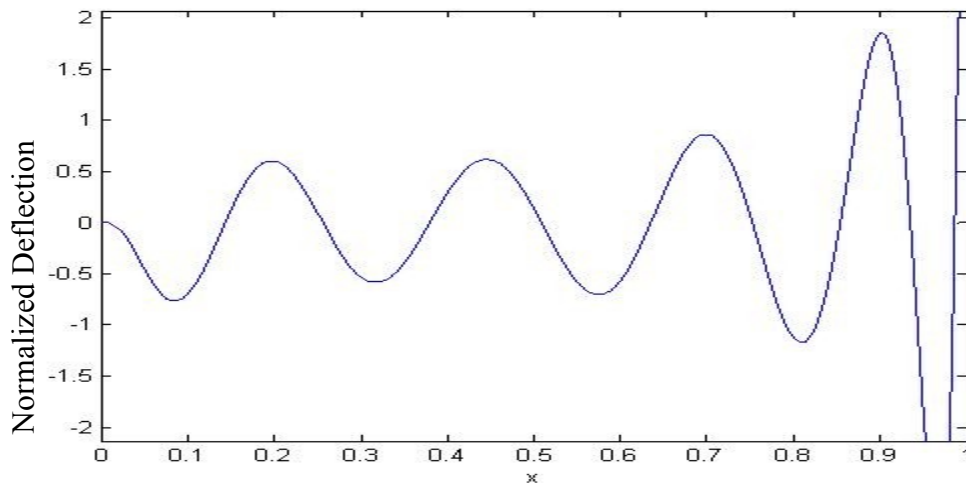
Figure 2.11: Mode 10 of cantilever beam using Rayleigh-Ritz method

The natural frequency of cantilever at each mode can be calculated by following expression.

$$\omega = \frac{C^2}{l^2}\sqrt{\frac{EI}{\mu}}$$

(2.26)

Chapter 3: Natural frequencies and mode shapes of a rectangular plates

When the width of a microcantilever is significant, it can be considered as a cantilever plate. Plates are used in many micro-electro-mechanical systems such as thin membranes of micro pump [5], circular membranes of high temperature pressure sensors [18, 52]. In this chapter, a brief literature review is provided on free vibration analysis of plates. Eigen value analysis of a square plate, clamped at all edges is presented using Rayleigh Ritz method.

3.1   Free vibration of rectangular plates

Leissa [45] has given a review of vibration of plates. H.L. Chen et al [14] performed free vibration analysis of rectangular plates using Bessel function method. Chow et al. [43] developed a general numerical method for estimation of vibration response of symmetrically laminated rectangular composite plates. He used orthogonal polynomials in Rayleigh-Ritz method to obtain eigen values and mode shapes of these plates.

Nair and Rao [44] used finite element method to find natural frequencies of rectangular plates. Beam characteristics functions were used to study plate vibration in Rayleigh-Ritz method by Leissa [45]. It includes analytical solutions for various shapes of plate. The boundary characteristic orthogonal polynomials suggested by Bhat [11] in Rayleigh-Ritz method are used in this report. These functions have already been used by several authors [46, 47, 48, 52] and found to be providing excellent results. For a rectangular plate, there are eight boundary conditions for each case. A plate fully clamped from all sides is considered in the present report.

3.2 Equation of motion of plate

The free vibration equation of motion of a rectangular plate can be expressed as follows.

$$D\nabla^4 w + \rho h \frac{\partial^2 h}{\partial t^2} = 0 \tag{3.1}$$

where ∇^4 is the biharmonic differential operator.

$$\nabla^4 = \nabla^2 . \nabla^2$$

$$\nabla^2 = \frac{\partial^2}{\partial x^2} + \frac{\partial^2}{\partial y^2}$$

$$D = \frac{Eh^3}{12(1-v^2)}$$

3.2.1 Eigen value analysis: Clamped-Clamped plate

The assumed deflection of a rectangular plate can be expressed as follows.

$$Y(x, y) = \sum_m \sum_n C_{mn} \Phi(x) \varphi(y) \tag{3.2}$$

where $\Phi(x)$ and $\varphi(y)$ are functions satisfying boundary conditions in x and y directions respectively.

Table 3.1 shows boundary conditions for a fully clamped rectangular plate.

Table 3.1: Boundary conditions for a fully clamped rectangular plate.

x=0	Y=0	$\dfrac{d^2Y}{dx^2}=0$
x=1	Y=0	$\dfrac{d^2Y}{dx^2}=0$
y=0	Y=0	$\dfrac{d^2Y}{dx^2}=0$
y=1	Y=0	$\dfrac{d^2Y}{dx^2}=0$

3.2.2 Kinetic and potential energies of the plate

$$KE = \frac{1}{2}\rho h a b \omega^2 \int_0^1\int_0^1 y^2(x,y)dxdy \tag{3.3}$$

$$PE = \frac{1}{2}\frac{D}{a^3\alpha}\int_0^1\int_0^1 [y_{xx}^2 + \alpha^4 y_{yy}^2 + 2\upsilon\alpha^2 y_{xx}y_{yy} + 2(1-\upsilon)\alpha^2 y_{xy}^2]dxdy \tag{3.4}$$

where ρ is density of the plate material, a and b are plate dimensions, h is its thickness, D is flexural rigidity of the plate, α is the side ratio a/b, υ is Poisson's ratio.

$$D = \frac{Eh^3}{12(1-\upsilon^2)} \tag{3.5}$$

Following functions satisfying boundary conditions for a square plate clamped at all edges are considered.

38

$$\phi(x) = x^2 - 2x^3 + x^4 \tag{3.6}$$

$$\varphi(y) = y^2 - 2y^3 + y^4 \tag{3.7}$$

Above polynomials are first made orthonormal using Equation (2.22) and further orthogonal polynomials are found by using Gram-Schmidt process described in section 2.3.2. Following are the orthogonal polynomials produced from $\Phi(x)$ and $\varphi(y)$.

$$\phi_0(x) = 25.09(x^2 - 2x^3 + x^4) \tag{3.8}$$

$$\phi_1(x) = 499.28(x - 1/2)(x^2 - 2x^3 + x^4) \tag{3.9}$$

$$\varphi_0(x) = 25.09(y^2 - 2y^3 + y^4) \tag{3.10}$$

$$\varphi_1(y) = 499.28(y - 1/2)(y^2 - 2y^3 + y^4) \tag{3.11}$$

Mass and stiffness matrices have been formed in Matlab using above equations of kinetic and Potential energies and following modes shapes have been obtained.

Frequency parameters of a square plate clamped at all edges for first four modes using above orthogonal polynomials compared with those from [11] for side ratio 1 are as follows.

3.2.3 Results and discussion

Mode shapes are presented four first four modes of the plate.

Table 3.2: Frequency parameters of clamped square plate using Rayleigh-Ritz and comparison with those from [11]

Mode no(m,n)	Present work	Analysis [11]
(1,1)	35.9855	35.9855
(2,1)	73.3947	73.395
(1,2)	73.3947	73.395
(2,2)	108.2179	108.22

Figure 3.1, Figure 3.2, Figure 3.3 and Figure 3.4 show first four modes plotted for clamped-clamped plate by using Rayleigh-Ritz method.
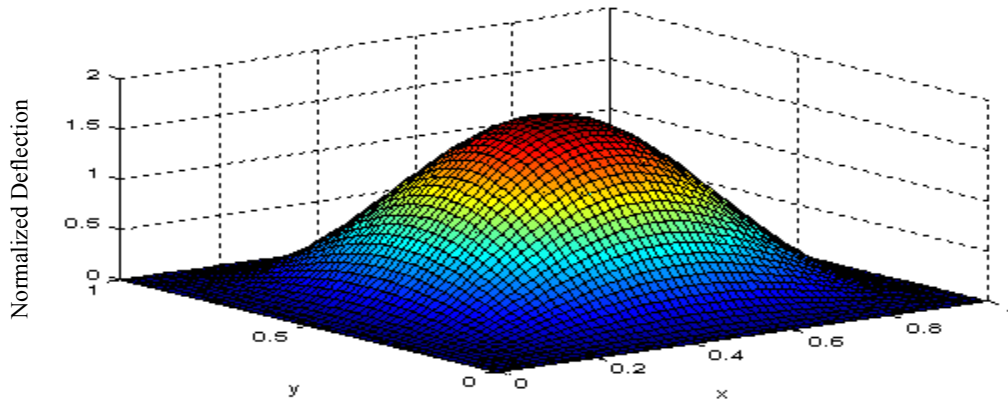
Figure 3.1: Mode (1,1) of clamped square plate using Rayleigh-Ritz method
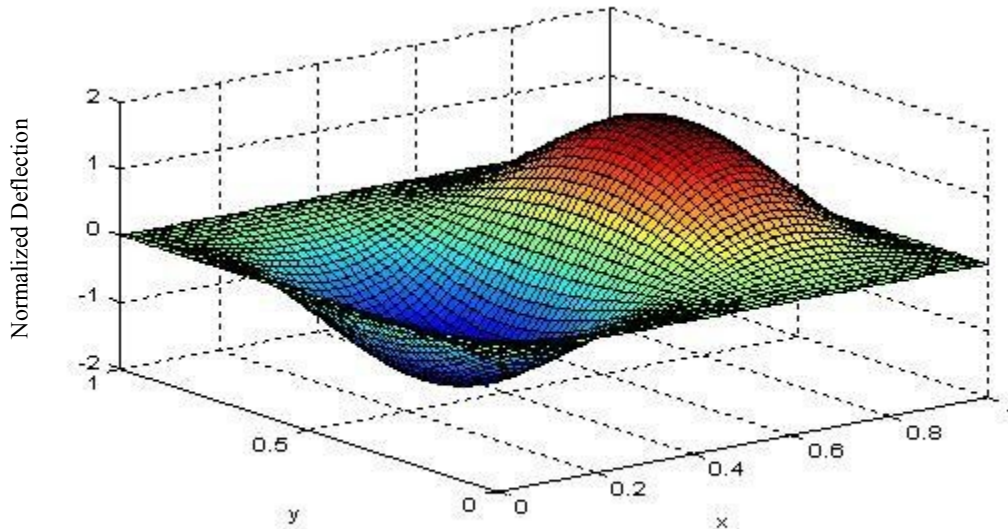
Figure 3.2: Mode (1,2) of clamped square plate using Rayleigh-Ritz method
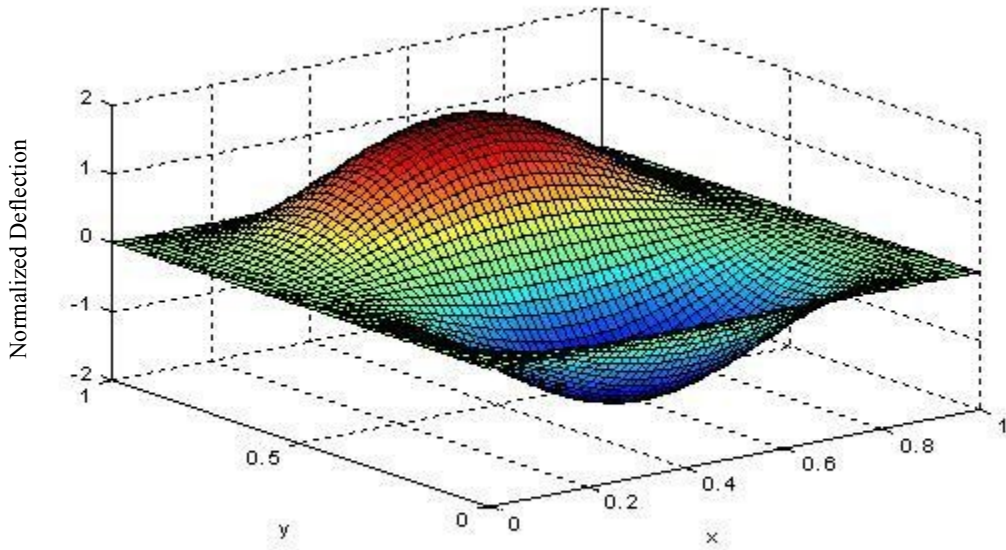
Figure 3.3: Mode (2,1) of clamped square plate using Rayleigh-Ritz method
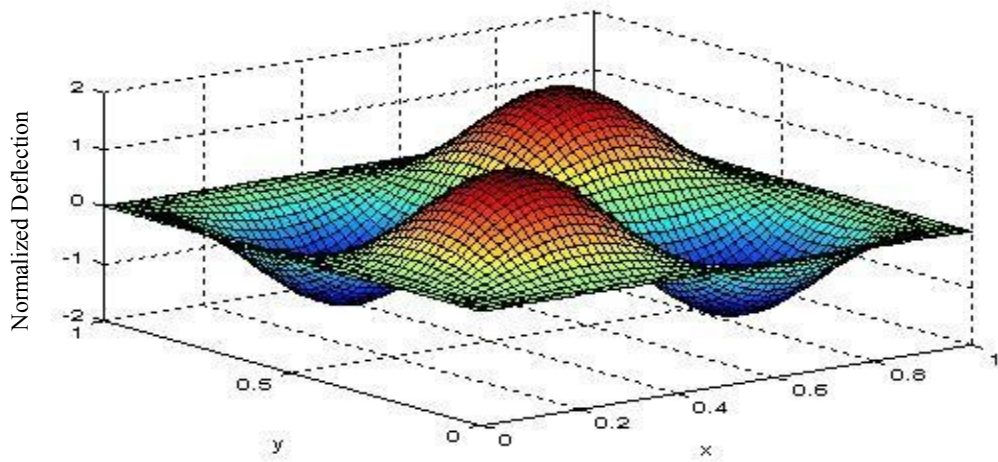
Figure 3.4: Mode (2,2) of clamped square plate using Rayleigh-Ritz method

Chapter 4: Dynamic modeling of microcantilever

The dynamics of the micro cantilever vibrating under the action of fluid forces can be exploited to develop sensors under fluid-structure interaction conditions to measure fluid properties. Generally, resonant frequencies of these cantilevers can be related to system parameters. The present chapter deals with modeling of Euler-Bernoulli beams in order to solve forced vibration problems under fluid-structure interaction problems.

4.1   Forced vibration of beams

Any external force acting on a flexible object tends to change its response. The external force can be electrostatic [10], mechanical force, or fluid pressure as considered in the present study. These forces can be harmonic, periodic or random in nature. The solution of these problems poses formidable challenges depending on the nature of the force. The force acting on the beam can be along the axial or the transverse direction. The present work is limited to forces acting on the beam in the transverse direction.

4.1.1 Governing Equation

The governing equation of motion of beam [17] with an external force in transverse direction can be expressed by Euler-Bernoulli equation as

$$EI\frac{\partial^4 y(x,t)}{\partial x^4} + \rho A\frac{\partial^2 y(x,t)}{\partial t^2} = P(x,t)$$

(4.1)

where P(x,t) is an external force per unit length acting on the beam.

Above equation is solved using mode-summation method as explained in following section.

4.1.2 Mode-summation method

According to mode-summation method, the solution of the above Equation (4.1) is assumed to be a linear combination of the normal modes of the beam as

$$y(x,t) = \sum_{i=1}^{n} Y_i(x) q_i(t)$$ (4.2)

where $Y_i(x)$ are the normal modes of vibration of the beam.

Replacing y in Equation (4.1) by Equation (4.2)

$$EI \sum_{i=1}^{n} Y_i'''(x) * q_i(t) + \rho A \sum_{i=1}^{n} Y_i(x) \ddot{\,}'(x,t)$$ (4.3)

It is assumed that the force is uniform and is sinusoidal, given by

$$P(x,t) = P_0(x) \sin(\omega t)$$ (4.4)

From the condition of orthogonality,

$$\int_0^l \rho A Y_i(x) Y_j(x) dx = 0 \qquad\qquad i \neq j$$

(4.5)

$$\int_0^l \rho A Y_i(x) Y_j(x) dx = 1 \qquad\qquad i = j$$

Using Equation (4.4) in Equation (4.3) and multiplying by $Y_j(x)$ on both sides;

$$\int_0^l EI(\sum_{i=1}^{n} Y_i'''(x) q_i(t)) Y_j(x) dx + \int_0^l \rho A(\sum_{i=1}^{n} Y_i(x) \ddot{\,} \, \quad)dx = \int_0^l P_0 \sin(\omega t) Y_j(x) dx$$ (4.6)

Considering the ith mode and removing the summation sign,

44

$$\int_0^l EIY_i'''(x)Y_i(x)q_i(t)dx + \int_0^l \rho A Y_i(x)Y_i(x)\ddot{} \quad = \quad \overline{P}_i\sin(\omega t); \quad i=j \tag{4.7}$$

where $\overline{P}_i = \displaystyle\int_0^l P_0 Y_i(x)dx$ is the modal force.

The first term in Equation (4.7) can be re-written as follows.

$$Y_i'''(x) = (\omega_i)^4 Y_i(x)$$

Hence, we have

$$EI\omega_i^4\sigma_i^2 q_i(t) + \rho A\sigma_i^2 \ddot{} \qquad \sin(\omega t) \tag{4.8}$$

where $\sigma_i^2 = \displaystyle\int_0^l Y_i^2(x)dx$

Adding the damping term into above equation,

$$EI\omega_i^4 q_i(t) + C\dot{} \qquad \ddot{} \qquad \frac{\overline{P}\sin(\omega t)}{\sigma_i^2} \tag{4.9}$$

4.1.3 Matrix formation of the equation

Considering first n modes for a beam, the above Equation (4.8) can be expressed in a matrix form as follows.

$$\begin{bmatrix} M_1 & 0 & 0 & 0 \\ 0 & \ddots & & \\ 0 & 0 & \ddots & \\ 0 & 0 & 0 & M_n \end{bmatrix}\begin{bmatrix} \ddot{} \\ \\ \\ \ddot{} \end{bmatrix} \cdots \begin{bmatrix} \\ \end{bmatrix} \cdots \begin{bmatrix} & 0 & 0 \\ 0 & \ddots & 0 \\ 0 & \ddots & \\ 0 & EI\omega_n^4 \end{bmatrix}\begin{bmatrix} q_1 \\ - \\ - \\ q_n \end{bmatrix} = \begin{bmatrix} \dfrac{\overline{P}_1\sin(\omega t)}{\sigma_1^2} \\ \vdots \\ \vdots \\ \dfrac{\overline{P}_n\sin(\omega t)}{\sigma_n^2} \end{bmatrix}$$

where

45

$$K = E * I * \omega^4$$

$$M = \rho * A$$

The matrix form can be summarized as follows.

$$M = \begin{bmatrix} (\rho A)_{1\times1} & 0 & \cdots & & 0 \\ 0 & \ddots & & & \vdots \\ \vdots & & \ddots & & \\ 0 & \cdots & & & \rho A)_{n\times n} \end{bmatrix}$$

$$C = \begin{bmatrix} (C)_{1\times1} & 0 & \cdots & \\ 0 & \ddots & & \vdots \\ \vdots & & \ddots & \\ 0 & \cdots & & C)_{n\times n} \end{bmatrix}$$

$$K = \begin{bmatrix} EIw^4_{1\times1} & 0 & \cdots & \\ 0 & \ddots & & \vdots \\ \vdots & & \ddots & \\ 0 & \cdots & & EIw^4_{n\times n} \end{bmatrix}$$

$$p = \begin{bmatrix} \dfrac{\bar{P}_i \sin(\omega t)}{\sigma_1^2} \\ \vdots \\ \vdots \\ \dfrac{\bar{P}_n \sin(\omega t)}{\sigma_n^2} \end{bmatrix}$$

$$[M]\{\ddot{q}, \quad \dot{q}, \quad q\} = \{p\} \tag{4.10}$$

The matrix form of the equation consists of mass matrix, damping matrix and stiffness matrix. It can be solved for q which is time history of the displacement of the beam. The following section explains the method of solution adopted to solve Equation (4.10).

$$\left.\begin{array}{cccc} \ddot{} & & & \end{array}\right][q][M]^{-1} \tag{4.11}$$

The q(t) obtained from above equation can be used in Equation (4.2) in order to obtain the deflection response of the beam.

First four modes are considered to obtain the deflection response of micro cantilever.

The final deflection can be expressed as follows.

$$Y(x,t) = \sum_{i=1}^{4} \phi_i q_i \tag{4.12}$$

4.1.4 Damping

In dynamic systems, damping is a phenomenon in which Mechanical energy is dissipated from the system. Damping can be present in various forms in a dynamic system. The knowledge of these forms and their level is important in order to understand the behavior of the system. Despite having a large literature on damping, there is no single universally accepted model for total damping present in a system since it is not possible to isolate various types of damping(material, structural and fluid) [33]. Damping can be expressed by various quantities such as specific damping coefficient, loss factor, Q-factor or damping ratio.

In the present study, damping matrix is achieved by using an approximate damping model reported for microcantilevers in [54]. The linear damping model is described in the following section.

Approximate damping coefficient C for microcantilever with rectangular cross section is defined as

47

$$C = (1.45 + 2.06\gamma)\pi\mu$$

(4.13)

Above expression has been obtained in [54] validating numerical analysis with experimental results. The expression has been expressed by carrying out experiments on microcantilevers of different sizes at different resonant frequencies tested for damping coefficients.

In the above equation, γ is a dimensionless parameter defined as

$$\gamma = \frac{width}{\alpha}$$

(4.14)

where α is a function of beam dimensions and fluid parameters expressed as follows.

$$\alpha = \sqrt{\frac{2\mu}{\rho\omega}}$$

(4.15)

where μ and ρ are fluid viscosity and fluid density. Further, ω is the resonant frequency of the beam.

The damping matrix is obtained by using above model with the present dimensions of beam and fluid parameters.

4.1.4.1 Fluid dependent damping

When a structure is vibrating under the action of a flowing fluid, the relative motion between a structure and fluid causes energy dissipation called as fluid damping. The damping effect in a fluid-structure interaction is produced by the boundary layer effects at the interface of fluid and structure. According to the damping model described above, Fluid damping is a function of viscosity of fluid, density of fluid and the dimensions of the structure.

Also, different types of damping associated with fluid flow can be found in literature. Pettigrew and Knowles [33] included an additional two phase damping term in fluid damping in flow

induced vibration in case of heat exchanger tubes. In his model, following relation can be found to determine total damping in a fluid-induced vibrating system.

$$\zeta = \zeta_s + \zeta_v + \zeta_{fd} + \zeta_{tp}$$

(4.16)

where ζ is the total damping ratio, ζ_s, ζ_v, ζ_{fd}, ζ_{tp} are damping ratios associated with structural damping which is friction damping at the joints, viscous damping which is present at the contact of tube to fluid, fluid damping and two phase damping, respectively.

4.1.5 Modeling in Simulink

Simulink offers a great variety of tools to solve problems involving dynamic systems. Different types of solvers are offered by Simulink based on the complexity of the problem and the type of numerical method. ode4 is a commonly used solver which is based on Runge Kutta Fourth Order. This Method has been chosen for the present problem to solve Euler-Bernoulli equation in time domain.

4.1.6 Fourth Order Runge-Kutta Solver

Runge-Kutta solver has been used to solve the differential equation. Theoretical approach of this method is presented below.

Consider a general Initial Value Problem on an Ordinary Differential Equation

$$f' = f(t, y)$$

(4.17)

$$f(t_0) = f_0$$

(4.18)

Runge Kutta Fourth Order method for solving f for the next step t_{n+1} is expressed by following equation.

$$f_{n+1} = f_n + \frac{1}{6}(g_1 + 2g_2 + 2g_3 + g_4)$$

(4.19)

where

$$g_1 = zf(t_n, f_n)$$

(4.20)

$$g_2 = zf\left(t_n \frac{1}{2}h, f_n + \frac{1}{2}g_1\right)$$

(4.21)

$$g_3 = zf\left(t_n + \frac{1}{2}z, f_n + \frac{1}{2}g_2\right)$$

(4.22)

$$g_4 = zf\left(t_n + z, f_n + g_3\right)$$

(4.23)

where $z = t_{n+1} - t$

The value of y_{n+1} is calculated at each time step using value of f from previous step.

The fixed step solver has been chosen for this particular problem since it offers the advantage of choosing desired time step as well as saving computation time [49]. On the other hand, variable time step solver takes more computation time since it automatically keeps on varying the size of the time step based on the rate of the change of the state and tolerance provided to achieve a specified level of accuracy over the course of simulation.

4.1.7 Discrete Fourier Transform

The results obtained in time domain are converted to frequency domain using the Discrete Fourier Transform. Fast Fourier Transform algorithm is used for this purpose. It is an efficient way to decompose a time domain response into different frequencies and their respective amplitudes.

The Fourier transform is defined as

$$F(f) = \int_{-\infty}^{\infty} f(t)e^{-i2\pi ft} dt$$

(4.24)

Above expression resolves the function f(t) into harmonic components F(f).

Numerical computation of Fourier transform requires discrete sample values of data in time domain, which is f (t). Numerically, the transform F(f) can only be computed at discrete values of s, which means, it can only provide discrete samples of the transform, F_r. If f (kT) and $F(rs_0)$ are the kth and rth samples of f(t) and F(f), respectively, and N_0 is the number of samples in the signal in a period T_0, then,

$$f_k = Tf(kT) = \frac{T_0}{N_0} f(kT)$$

(4.25)

and

$$F_r = F(rs_0)$$

(4.26)

where

$$s_0 = 2\pi F_0 = \frac{2\pi}{F_0}$$

Discrete Fourier Transform is given by

$$F_r = \sum_{i=1}^{n} f_k e^{-ir\Omega_0 k}$$

(4.27)

where

$$\Omega_0 = \frac{2\pi}{N_0}$$

4.1.8 Fast Fourier Transform

The Fast Fourier Transform is a DFT algorithm developed by Tuckey and Cooley in 1965 which reduces the number of computations from the order of N_0^2 to $N_0 \log N_0$. N_0 is the chosen to be the power of 2 in this algorithm.

4.1.9 Summary

This chapter describes theoretical modeling of Euler-Bernoulli equation using mode summation method. Further, it explains a method to solve it using Simulink.

Chapter 5: Validation and results

Several experiments on fluid-structure interaction of beams and plates can be found in literature. Shakhawat [19] performed an experiment on micro cantilever vibrating under the action of fluid. The fluid pressure and excitation frequencies of the fluid loading on the micro cantilever are obtained from this experiment. The following section describes briefly about the experimental set up and properties of micro cantilever [19].

One such application of flow induced vibration is sensing density of fluids with the help of frequency response of the cantilevers [1]. Density is one of the fundamental physical quantities required when the property or composition of a liquid sample is required to be determined in industrial processes. Density measurement can be a crucial parameter where gas leak is to be detected such as in automobiles and airplanes. Also, the detection and characterization of chemicals in liquid and gaseous state can be carried out using density measurement [1].

5.1   Experimental Set up: Review

The experiment [19] was performed to understand fluid-structure interaction of micro cantilevers under different flow rates and fluid pressures. The results included deflection response of micro cantilevers under the action of different fluid flows within micro chips.

Figure 5.1 shows the micro channel used in the experimental set up [19]. The micro cantilever was excited by fluid flow through the two inlets as shown. The size of the inlet of microchannel is 3.2×3.2 mm.
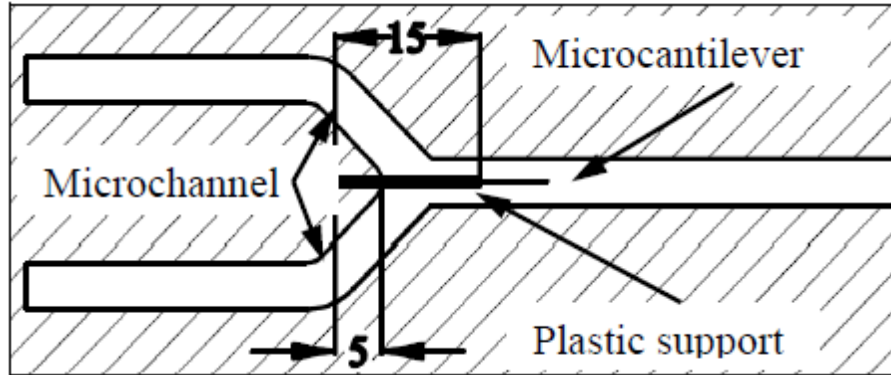
Figure 5.1: Micro cantilever assembled in a micro channel[19][Dimensions are in mm]

In the experimental set up, a peristaltic pump was employed for the fluid flow to take place through two inlets and pressure across two inlets were measured by using two pressure sensors across inlets. The data through the pressure sensors were obtained through a data acquisition board. The oscillatory flow produced by the pump acts as the dynamic loading on the micro cantilever.

5.1.1 Flow through the pump

Flow through a peristaltic pump takes due to the squeezing action of the tubes by rollers centrally distributed around a central disc. In the experiment, it was found that the flow through the pump takes place due to frequencies contributed by speed of the central disc as well as that due to the rollers. The experiment was performed with the help of Fluid XP. The density and viscosity of the fluid are $1029 \, kg/m^3$ and 4.5×10^{-3} Pa.s respectively. Figure 5.2 shows the frequency spectrum of the flow variation at 6 rpm speed of the pump. The frequency spectrums of pressure

loadings that were obtained experimentally by Shakhawat [19] are reviewed and used for the present study.
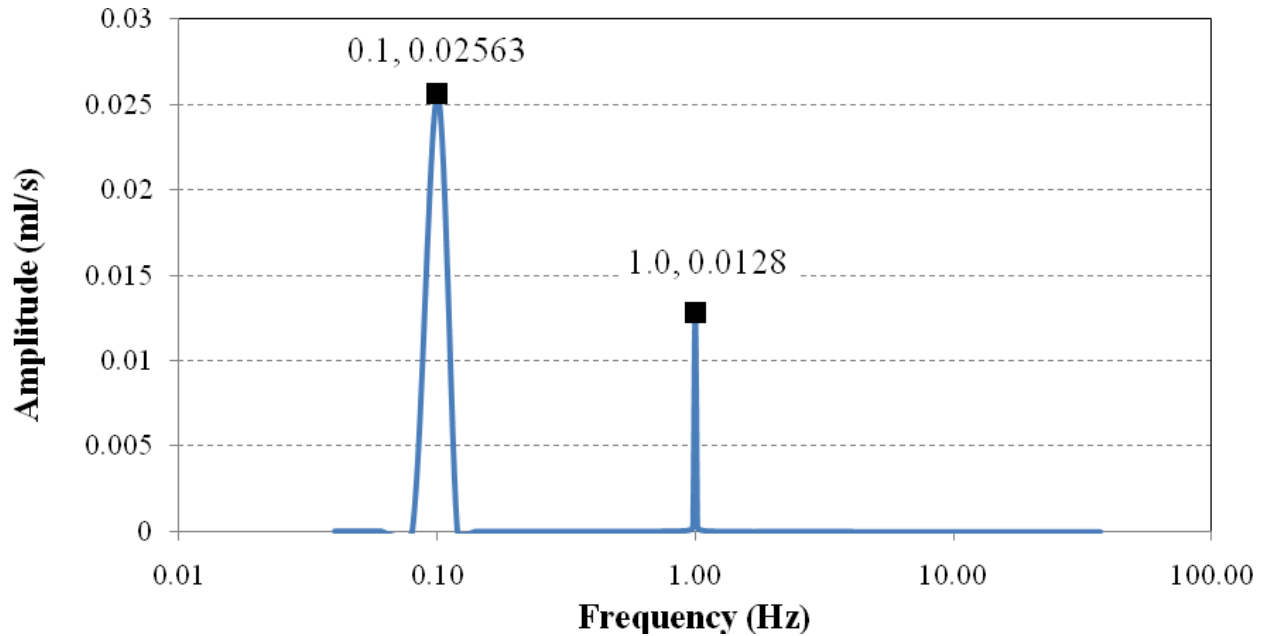
Figure 5.2:Frequency variation of the flow through the peristaltic pump [19]

The flow through the pump was found to be periodic consisting of two harmonic frequencies. These frequencies were corresponding to the angular velocities of the discs inside the pumps and to those of the rollers. Frequency of the flow is related to the angular velocity of the disc as follows.

$$f_1 = \frac{\omega}{2\pi} = \frac{N}{60}$$

$$f_2 = 10 f_1$$

where f = frequency of fluctuation

ω= angular velocity of the disc in rad/s

N= RPM of the disc

f_2 = Passing frequency of rollers

Thus, the pressure loading on the beam was found to be consisting of two pressure amplitudes associated with two harmonic frequencies.

$$\Delta P = P_1 \sin \omega_1 t + P_2 \sin \omega_2 t$$

(5.1)

where P_1 and P_2 are the pressure amplitudes corresponding to two harmonic frequencies.

The force acting on the cantilever can be assumed to be of the same form and can be expressed as follows.

$$F = f_1 \sin \omega_1 t + f_2 \sin \omega_2 t$$

(5.2)

In the present work, the values of pressure are taken from the experiment and used in the Euler-Bernoulli beam model in order to find the time history of the displacement of the tip of the cantilever.

5.2 Material and Dimensions of micro cantilever

The material of the micro cantilever used in the experiment was PVDF (Polyvinyl Fluoride). The material was chosen based on its availability in different sizes [19]. Micro cantilevers can be easily fabricated with PVDF. Also, it is light weight and flexible material. The micro channel was fabricated from PDMS using soft lithography [19]. The properties of PVDF material and microcantilever dimensions are summarized in Table 5.1 and Table 5.2.

Table 5.1: Mechanical Properties of PVDF material

Property	Value
Young's modulus	4×10^{9} N/m^2
Poisson's ratio	0.35
Density	1780 kg/m^3

Table 5.2: Dimensions of micro cantilever

Dimension	Value (m)
Length	7.0×10^{-3}
Width	2.1×10^{-3}
Thickness	28×10^{-6}

In the present work, above dimensions of the micro cantilever are used in the numerical model. The deflection response has been obtained for the six different cases of frequency and pressure taken from the experiment.

5.3 Results and Discussion

The deflection of the tip of micro cantilever under the action of two pressure components is presented in frequency domain. The results are compared for six different combinations of frequency and pressure that were experimentally determined by Shakhawat[19].

Figure 5.3, Figure 5.5, Figure 5.7, Figure 5.9, Figure 5.11 and Figure 5.13 show fluid pressure variation with respect to frequency in six different cases of the pump speed used during the

experiment. The variation of pressure has been obtained for the 3.2 mm hydraulic diameter of the microchannel. The fluid pressure and excitation frequency data are obtained from these figures for a particular fluid.
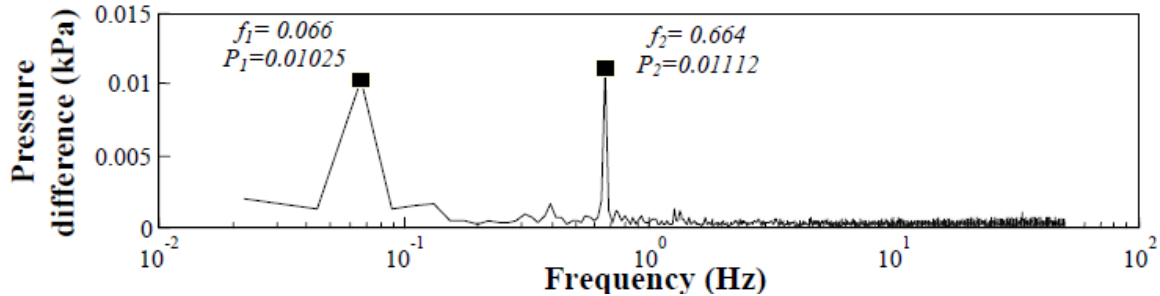
Figure 5.3: Variation of pressure with frequency at 4 RPM speed of the pump[19]

Deflection response of microcantilever provides an idea about its dynamic behavior to a particular frequency. Figure 5.4 shows deflection response in frequency domain obtained using Fast Fourier Transform. It shows two deflection amplitudes corresponding to two excitation frequencies. It can be seen that the deflection amplitude at f_2 is higher than that f_1. In Figure 5.3, [f_1, P_1] and [f_2, P_2] represent [frequency of excitation, amplitude] of fluid loading. The lower frequency is attributed to the angular motion of the central disc while the higher component of frequency can be attributed to the passing frequency of the rollers. The pressure of fluid downstream the cantilever has been measured using two pressure sensors at the inlet of the channel [19].

58
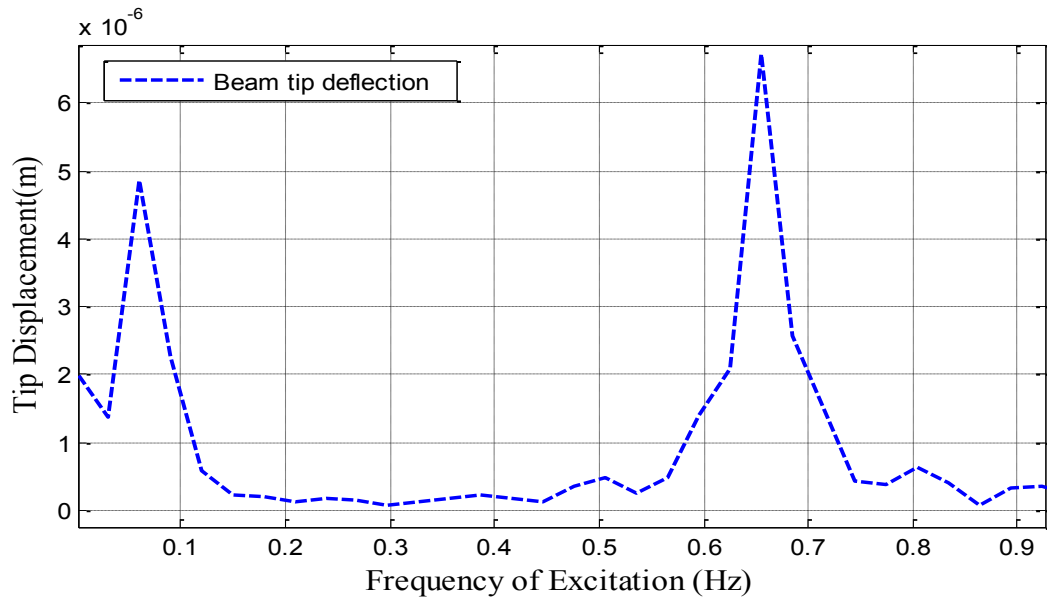
Figure 5.4: Deflection response of tip of microcantilever obtained using Numerical model at speed of the pump 4 RPM

Figure 5.4 shows tip deflection amplitudes of PVDF microcantilever obtained using Mode-Summation method. It shows deflections of the cantilever corresponding to the excitation frequencies f_1 and f_2 shown in Figure 5.3. Two excitation frequencies are 0.066 Hz and 0.66 Hz. The excitation frequencies obtained in Figure 5.3 correspond to 4 RPM speed of the pump used in the experiment. The result shows slightly higher deflection at higher frequency than that at lower frequency component.
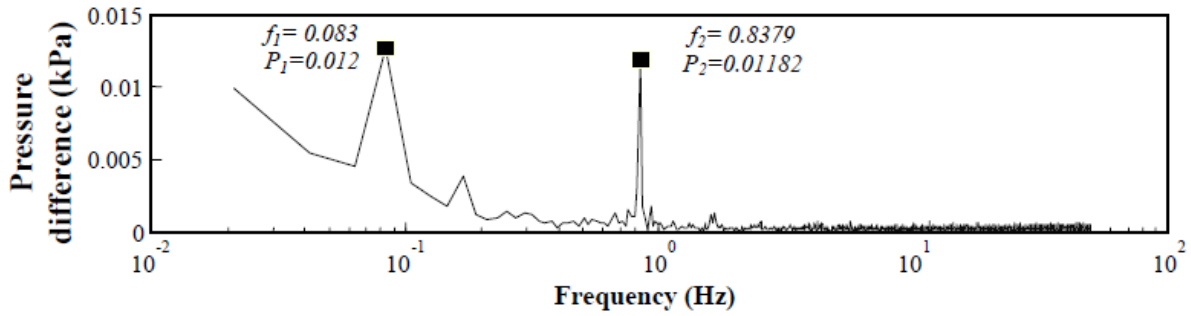
Figure 5.5: Variation of pressure with frequency at speed of the pump 5 RPM[19]

Figure 5.5 shows fluid pressure loading and excitation frequencies corresponding to speed of the pump 5 RPM. A slightly higher pressure loading can be observed in this case as compared to the previous one.
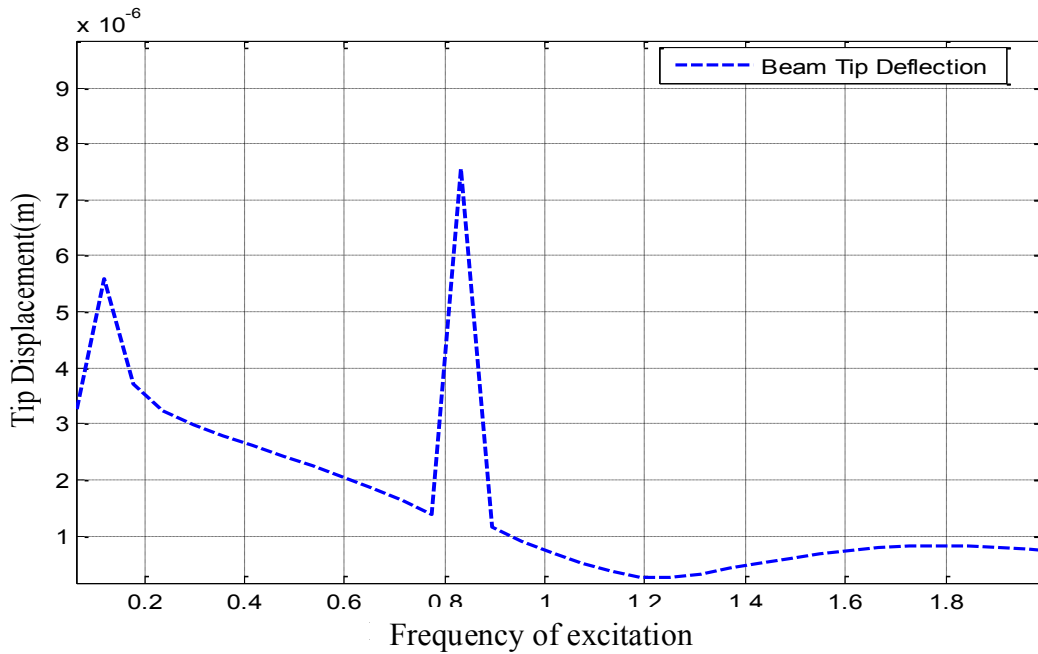
Figure 5.6: Deflection response of tip of micro cantilever using Numerical model at speed of the pump 5 RPM

Figure 5.6 shows that a little increase in the pressure loading and excitation frequency show increase in both the amplitudes of the beam. The excitation frequencies correspond to speed of the pump 5 RPM.
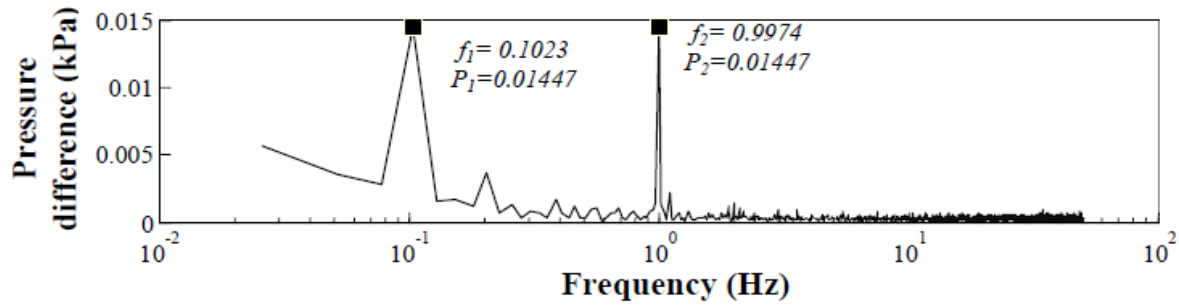
Figure 5.7: Variation of pressure with frequency corresponding to speed of the pump 6 RPM[19]

The fluid loading and excitation frequencies in Figure 5.7 correspond to 6 RPM speed of the pump.
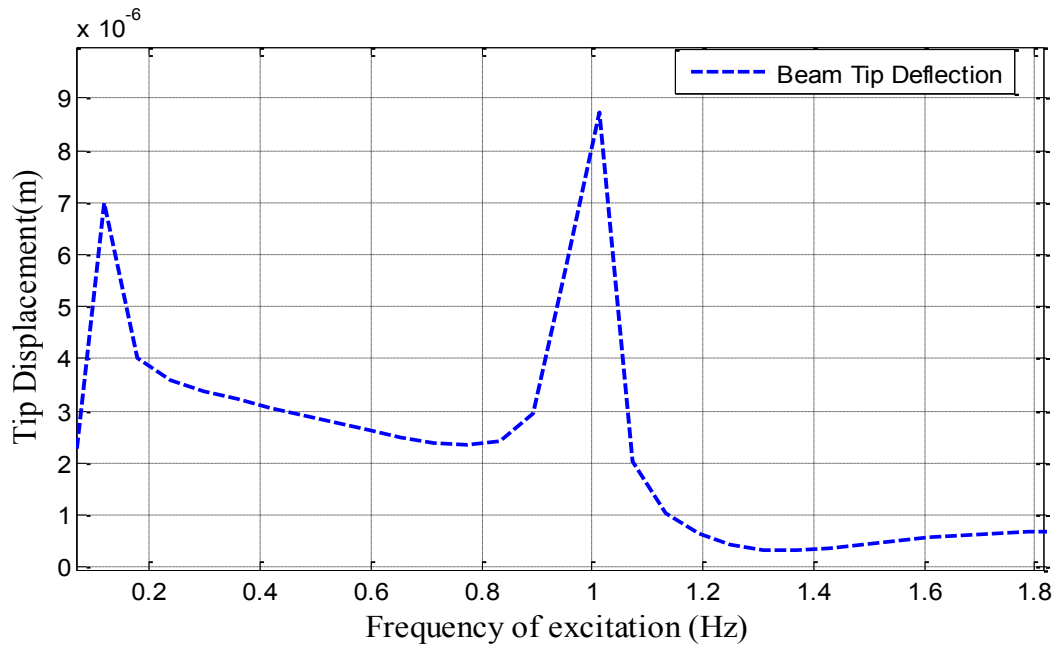
Figure 5.8: Deflection response of tip of micro cantilever using Numerical model at speed of the pump 6 RPM

61

Figure 5.8 shows deflection amplitudes at the pressure loading P₁ and P₂ shown in Figure 5.7.
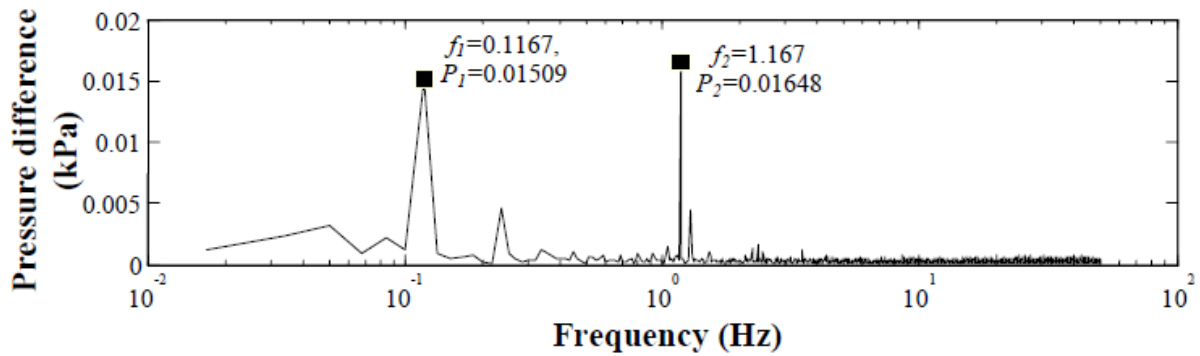
Figure 5.9: Variation of pressure with frequency corresponding to speed of the pump 7 RPM[19]

The excitation frequencies in Figure 5.9 correspond to 7 RPM speed of the pump.
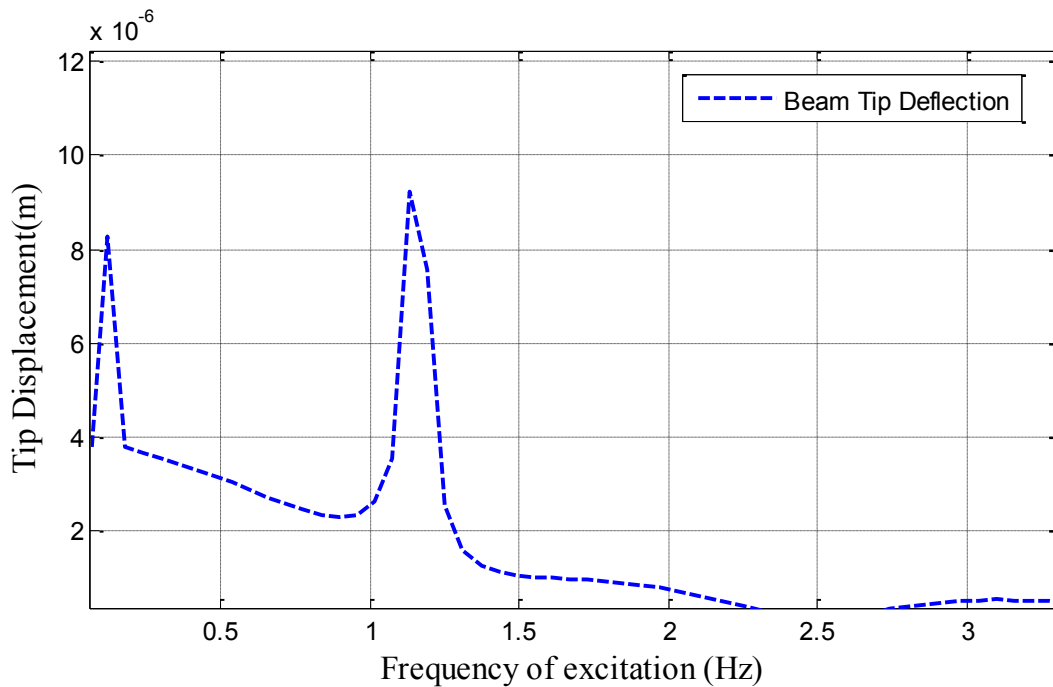
Figure 5.10: Deflection response of tip of micro cantilever using Numerical model at speed of the pump 7 RPM

Figure 5.10 shows frequency transform of tip displacement of the beam for pressure loading shown in Figure 5.9.
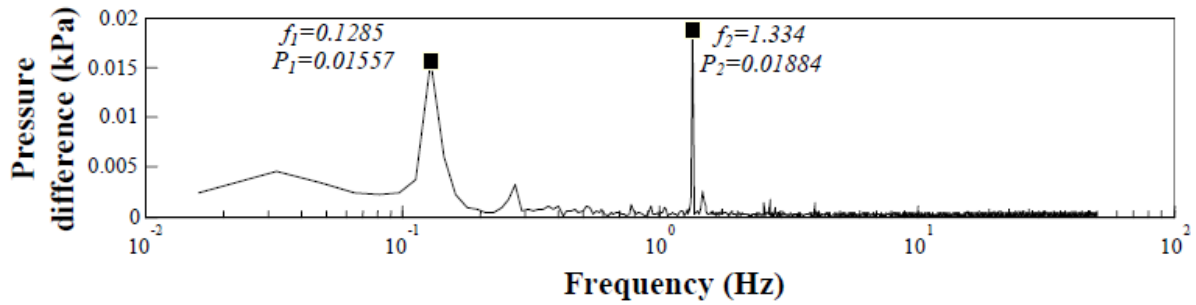
Figure 5.11: Variation of pressure with frequency corresponding to speed of the pump 8
RPM[19]

The pressure loading and excitation frequencies in Figure 5.11 correspond to 8 RPM speed of the

pump.
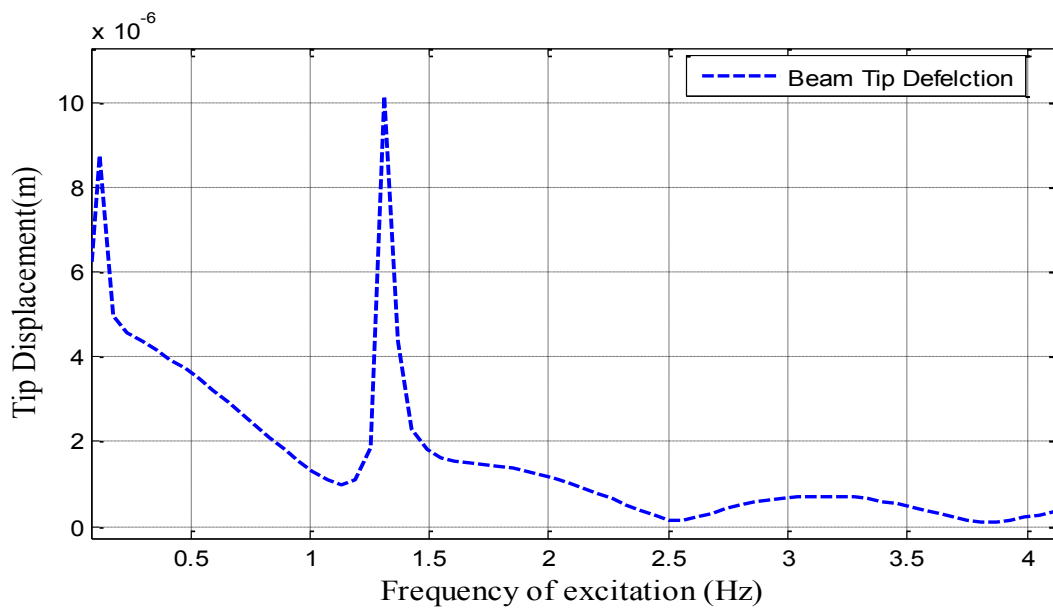
Figure 5.12: Deflection response of tip of micro cantilever using Numerical model at speed of
the pump 8 RPM

Figure 5.12 shows tip displacement of the microcantilever beam corresponding to the pressure

loading shown in Figure 5.11.
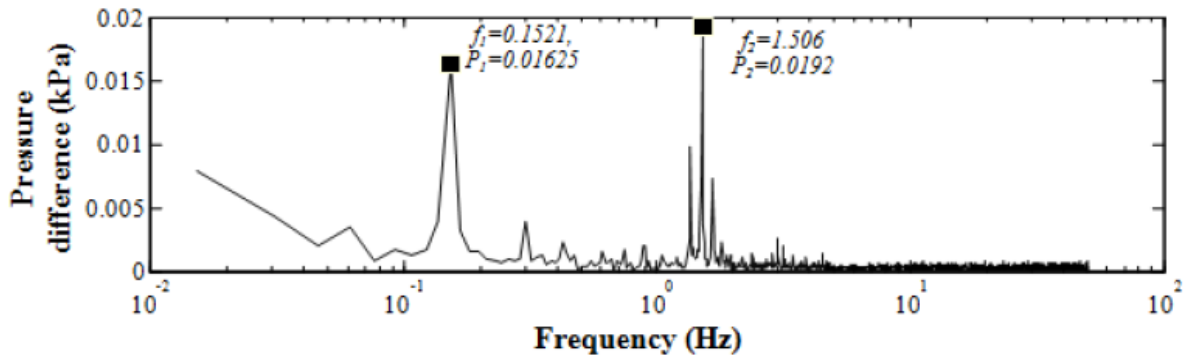
Figure 5.13: Variation of pressure with frequency corresponding to speed of the pump 9
RPM[19]

The pressure loading and excitation frequencies in Figure 5.13 correspond to speed of the pump
9 RPM.
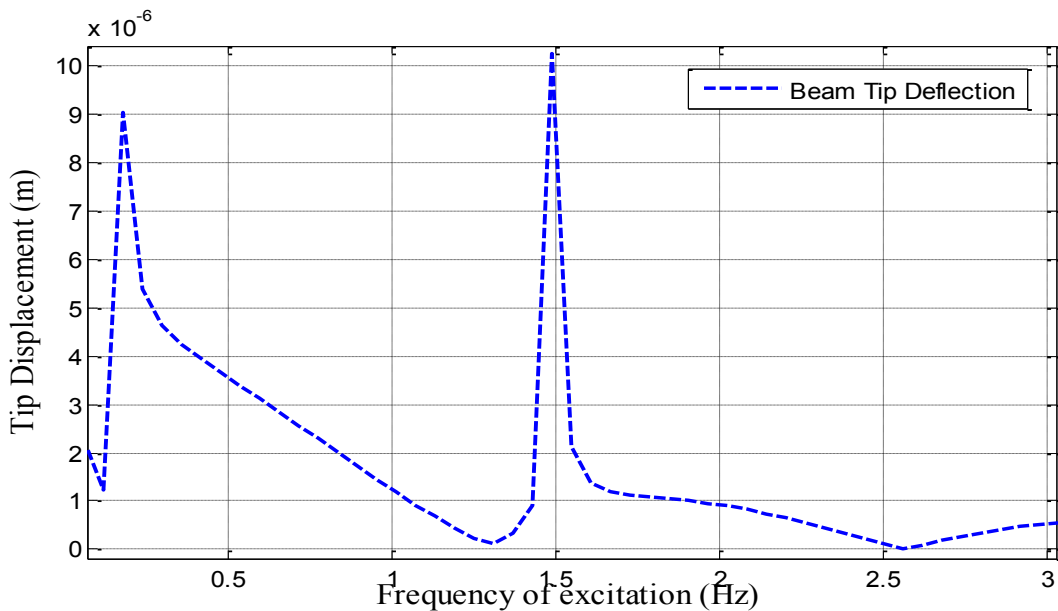
Figure 5.14: Deflection response of tip of micro cantilever using Numerical model at speed of
the pump 9 RPM

The predicted amplitudes of these six cases are compared with those found from the experiment [19]. The pressure of the fluid depends on the frequency of operation of the peristaltic pump. Amplitudes A_1 correspond to the frequency f_1 and amplitudes A_2 correpsond to the frequency f_2.

Figure 5.15 shows variation of fluid pressure with frequency as well as variation of amplitudes A_1 with frequency. It can be seen that the fluid pressure increases with the increase in the excitation frequency. The excitation frequency is a function of speed of the pump.
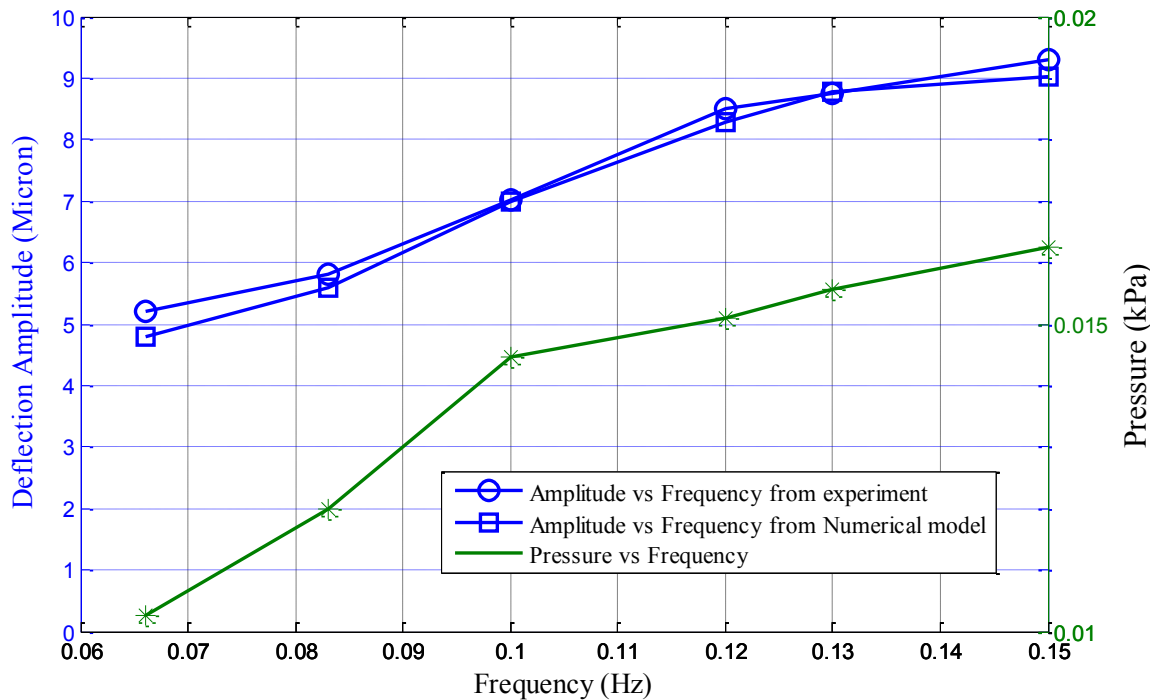
Figure 5.15:Comparison of deflection amplitudes A_1 from numerical model and experiment and variation of pressure with frequency

Deflection amplitudes A_1 from the numerical model and those from the experiment are compared in Figure 5.15. One can notice a close agreement between values predicted from the numerial model and the experimental values.
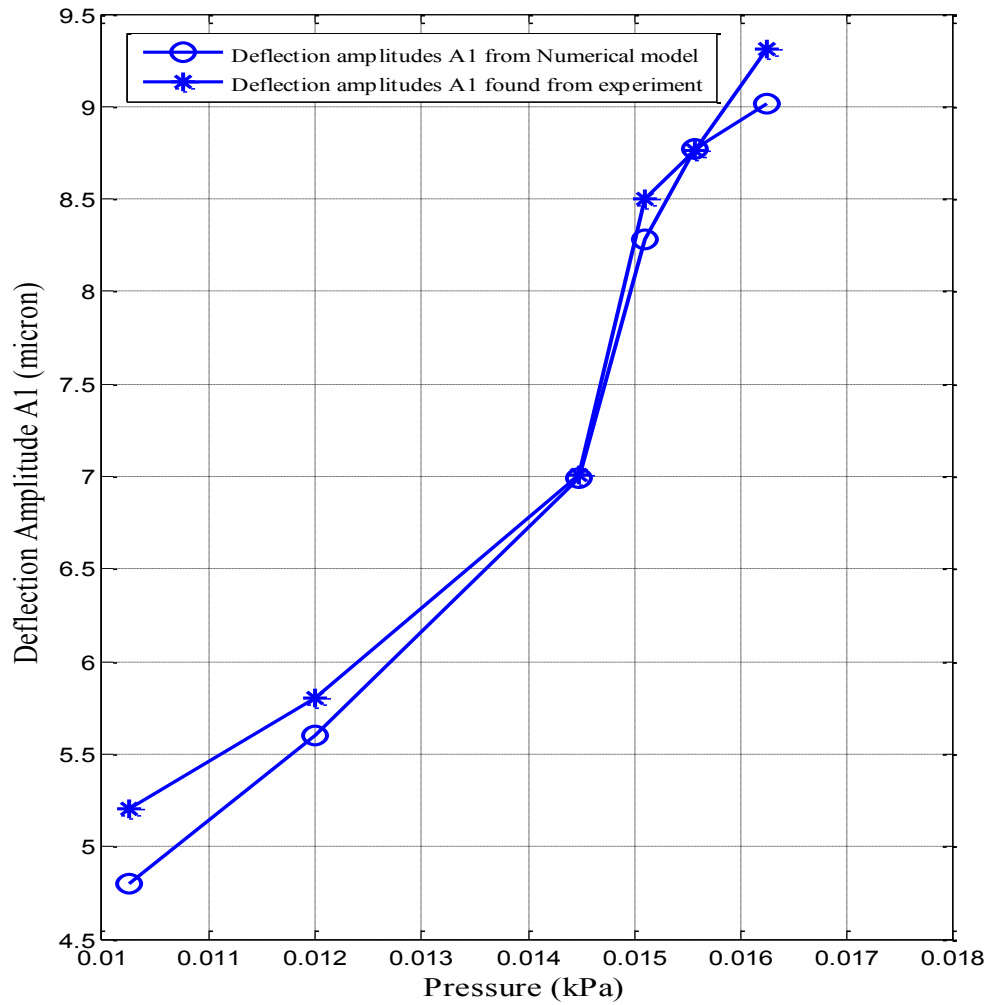
Figure 5.16: Variation of deflection amplitudes A_1 from numerical model and experiment with pressure P_1

Deflection amplitudes are plotted against pressure laoding in order to observe the effect of loading. Figure 5.16 shows variation of amplitude A_1 found from the numerical model with the fluid pressure from the experiment. It can be observed that the deflection amplitudes increase with increase in loading on the microantilever.
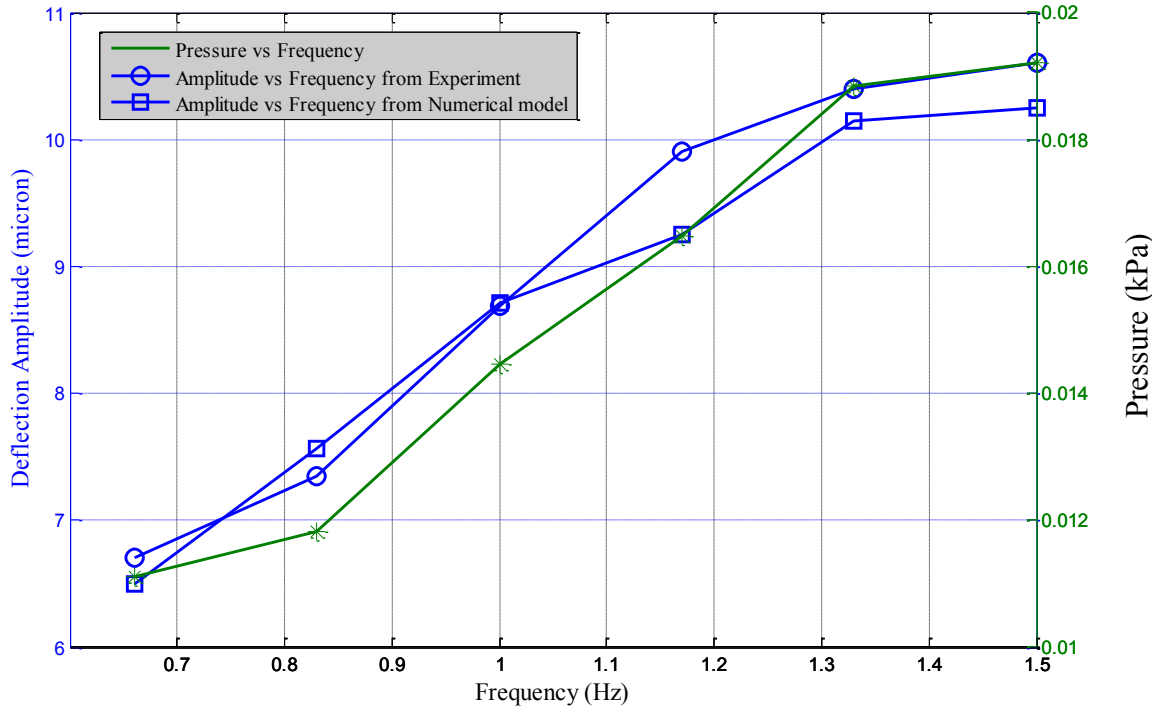
Figure 5.17: Comparison of deflection amplitudes A2 from numerical model and experiment and variation of pressure P2 with frequency

Similarly, deflection amplitudes A2 are compared with those from the experiment. Also, Figure 5.17 shows variation of fluid pressure loading with excitation frequencies. It can be observed that the pressure loading increases with increase in excitation frequency.

The deflection amplitudes were obtained in the experiment using Video Image Processing utilizing a CMOS camera [19].

The accuracy of the results obtained here depends upon the choice of number of undamped modes for the cantilever. Since the first natural frequency of the cantilever beam used in the present study is $f_1 = 120 \, Hz$ and the excitation frequencies ω_1 and ω_2 are close to 1 Hz, the first mode would provide significant contribution to the dynamic deflection of microcantilever.

Hence, considering four modes, the accuracy of the first mode is quite good while the other three modes may not be as accurate, is believed to be reasonable.
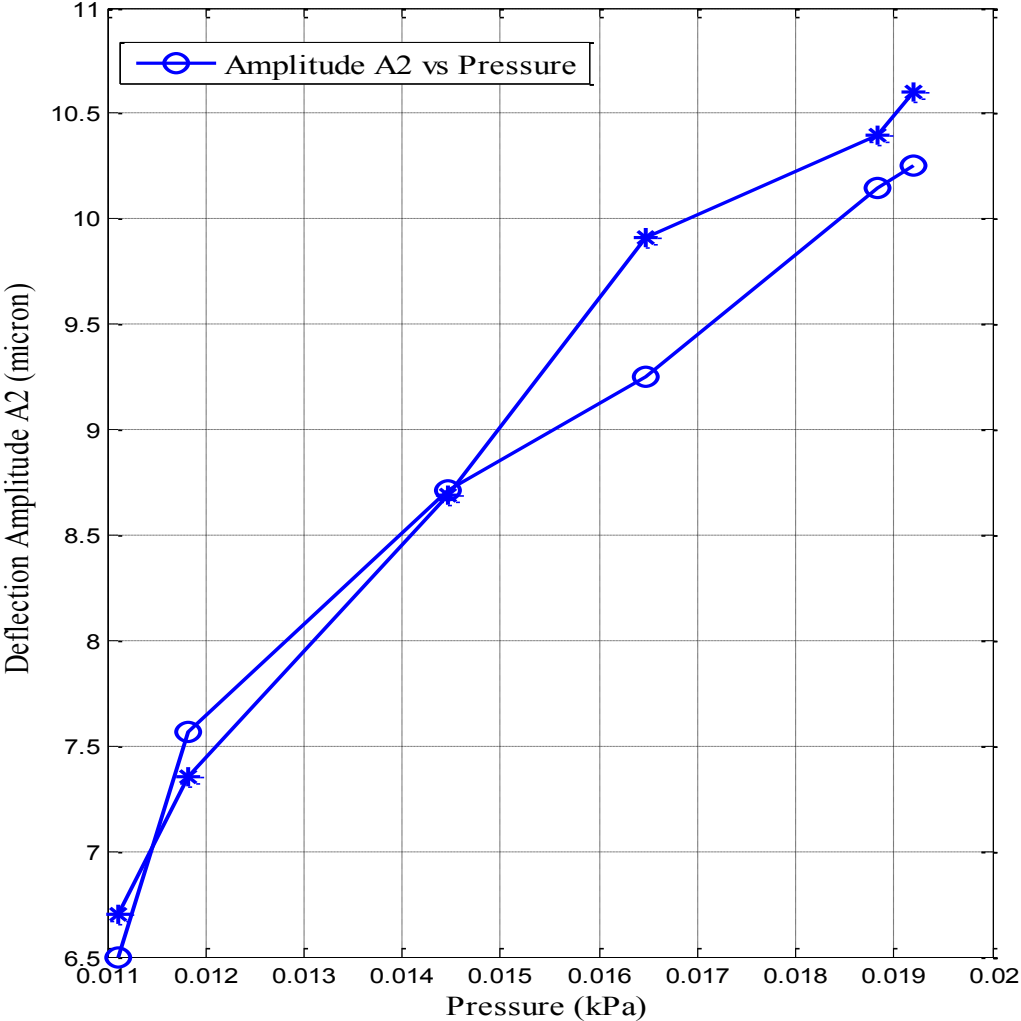
Figure 5.18: Variation of deflection amplitudes A₂ from numerical model and experiment with pressure

Figure 5.18 shows variation of amplitude A₂ found from the numerical model with the fluid pressure from the experiment. The deflection amplitudes can be seen to be increasing with the pressure loading as in the previous case.

5.4 Parametric Study on the Dynamics of microcantilever

Dynamics of a microcantilever can predominantly depend upon its shape and size. It can have various shapes such as rectangular, double legged or triangular with different aspect ratios. Different sizes of the micro cantilevers can have different sensitivities to the fluid loading while using them in sensing applications.

In this section, a parametric study is presented with different aspect ratios of rectangular micrcantilevers made of PVDF, subjected to a certain set of fluid loading and excitation frequency obtained using the experimental set up described in section 5.1. In a similar way, two deflection amplitudes are obtained using numerical model in order to analyze the effect of aspect ratio on the dynamic deflection of the microcantilever subjected to two harmonic frequencies of fluid loading. Table 5.3 shows widths and lengths chosen for the parametric study and corresponding aspect ratios. Thickness of the beam is 28 micron in all the cases.

Table 5.3: Geometrical parameters chosen for parametric study

Width (mm)	Length (mm) L			
w	2.5	5	7.5	10
	Aspect ratio (L/w)			
0.5	5	10	15	20
1	2.5	5	7.5	10
2	1.25	2.5	3.75	5
4	0.625	1.25	1.875	2.5

Table 5.4 shows values of pressure loading and excitation frequencies chosen for the paraemtric study.

Table 5.4: Pressure loading and excitation frequencies used in parametric study

	Pressure (kPa)	Frequency (Hz)
1	0.01625	0.15
2	0.0192	1.5

5.4.1 Results and Discussion

The results are obtained for the tip displacement of the microcantilever having different widths and lengths. The idea of presenting parametric study is to determine the deflection amplitudes for different dimensions of microcantilever. Deflection response results are presented for each combination of width and length of the beam shown in Table 5.3. The results are obtained using the numerical model described in Chapter 4.

Figure 5.19 - Figure 5.22 show frequency repsonse of microcantilevers with width 0.5 mm under the action of fluid loading. The lengths of the beam chosen are 2.5 mm, 5 mm, 7.5 mm and 10 mm. Two peaks can be observed corresponding to excitation freqiencies 0.15 Hz and 1.5 Hz in each figure. The increase in deflection amplitudes can be seen with longer beams.
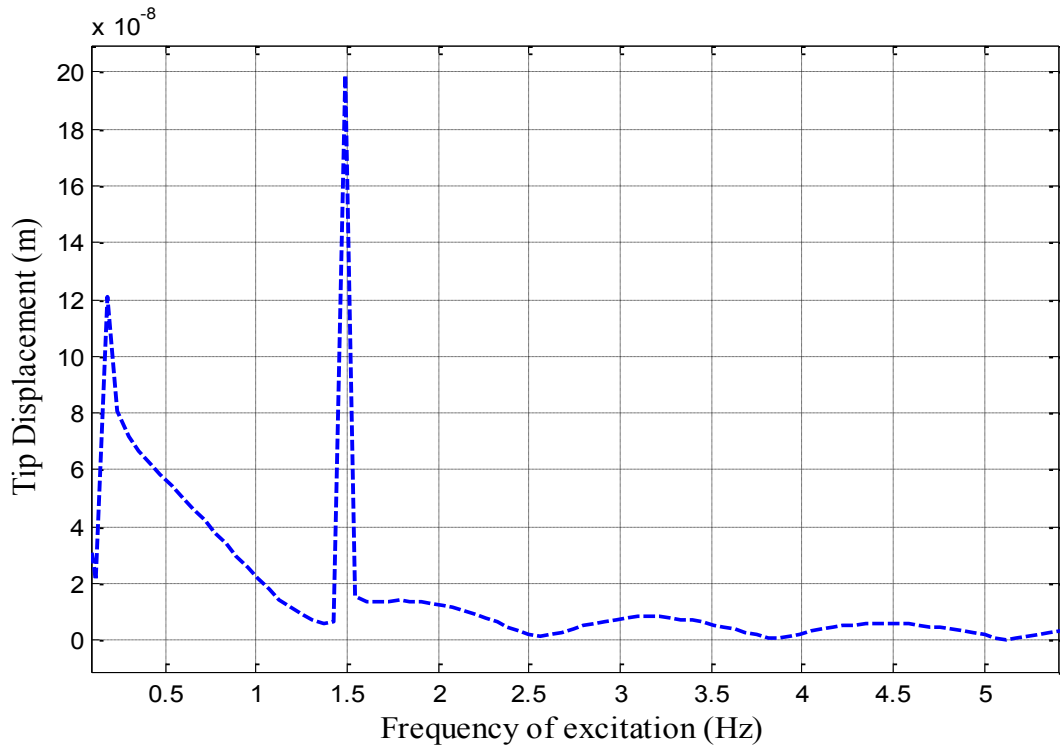
Figure 5.19: Tip deflection response of microcantilever 0.5 mm width X 2.5 mm length
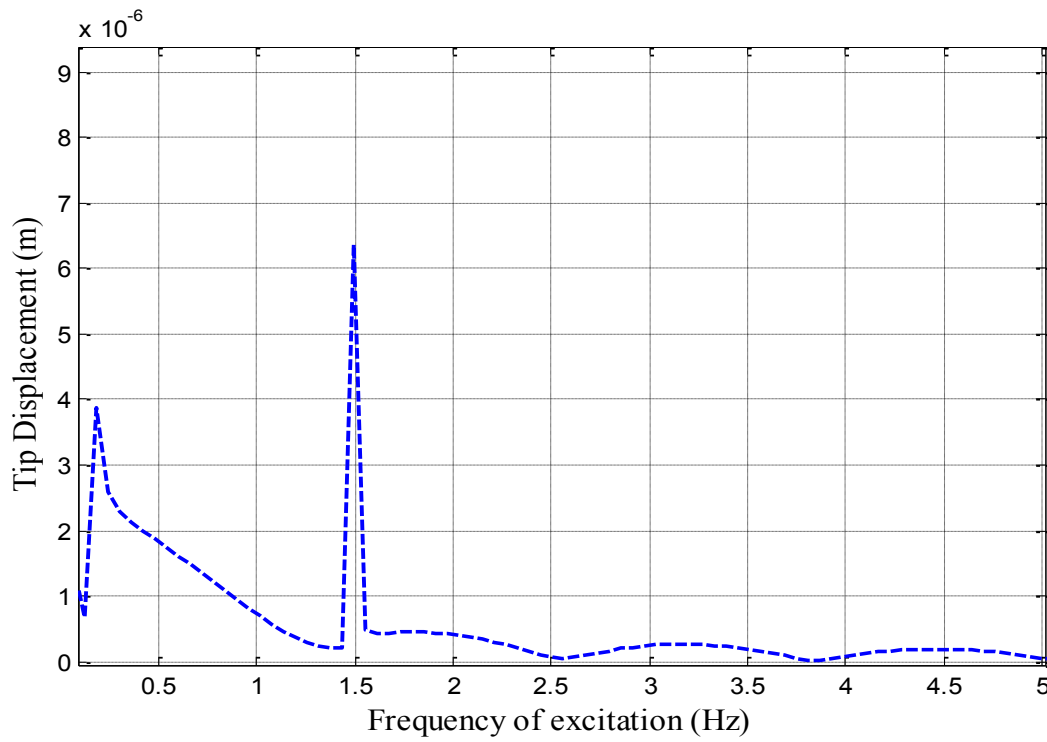
Figure 5.20: Tip deflection response of microcantilever 0.5 mm width X 5 mm length
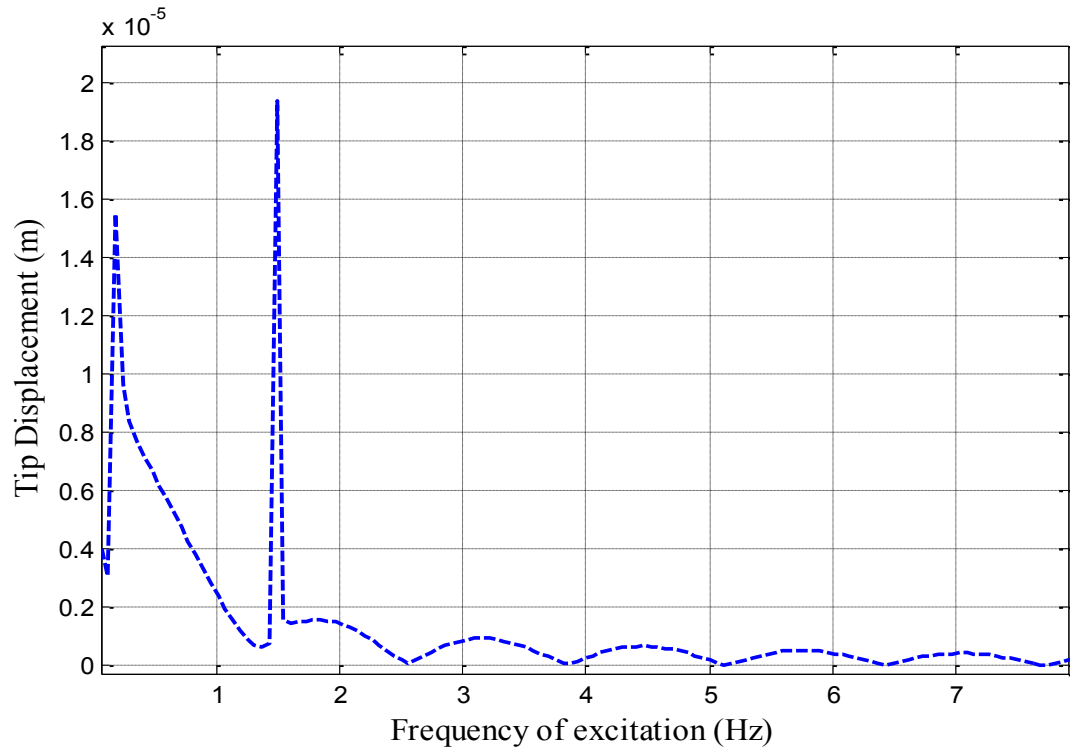
Figure 5.21: Tip deflection response of microcantilever 0.5 mm width X 7.5 mm length
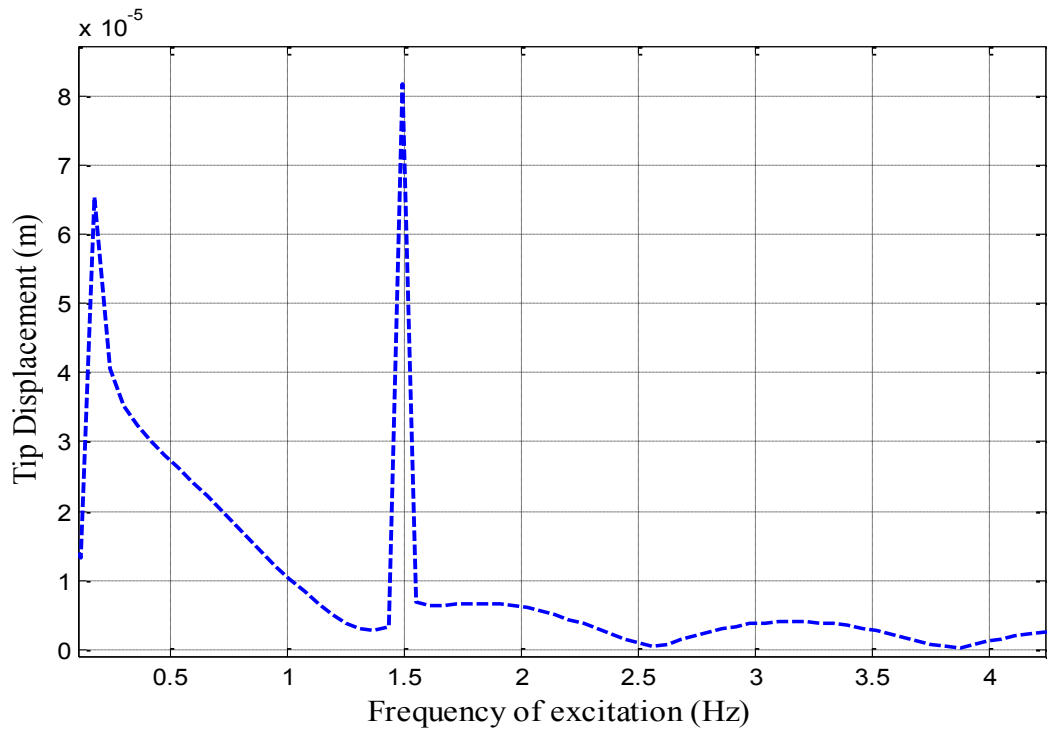
Figure 5.22: Tip deflection response of microcantilever 0.5 mm width X 10 mm length

Figure 5.23 - Figure 5.26 show deflection amplitudes of microcantilever having width 1 mm under the action of fluid loading.
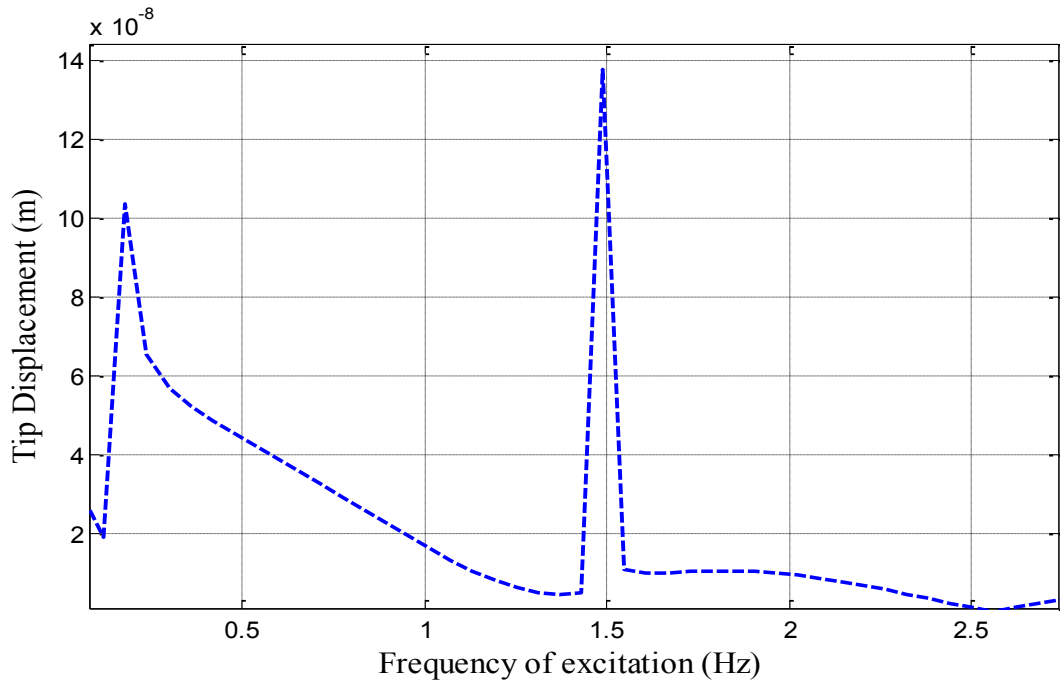
Figure 5.23: Tip deflection response of microcantilever 1 mm width X 2.5 mm length
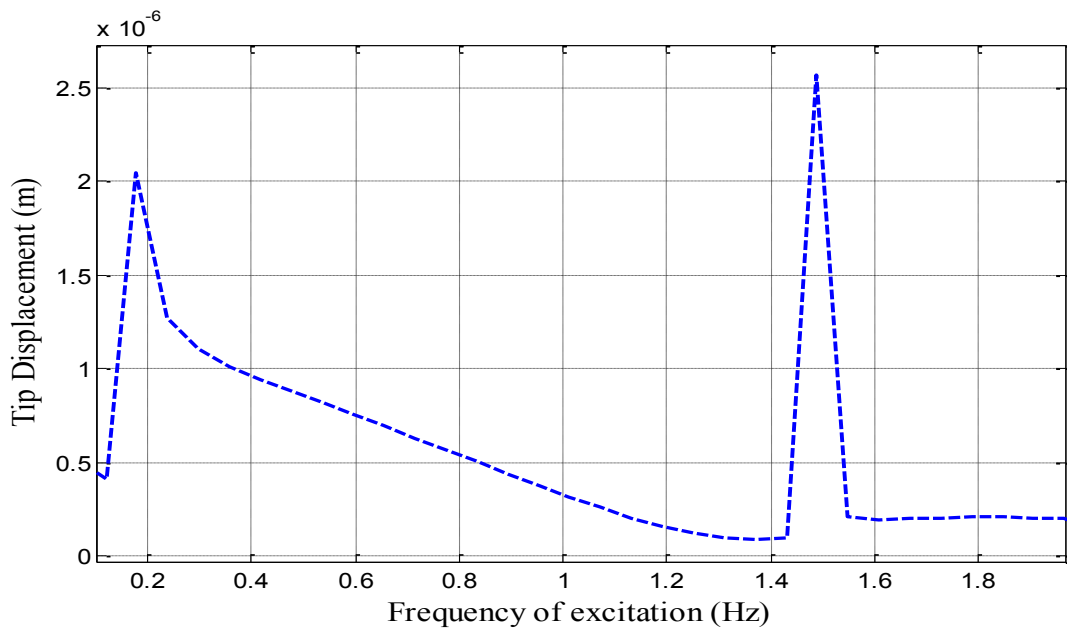
Figure 5.24: Tip deflection response of microcantilever 1 mm width X 5 mm length
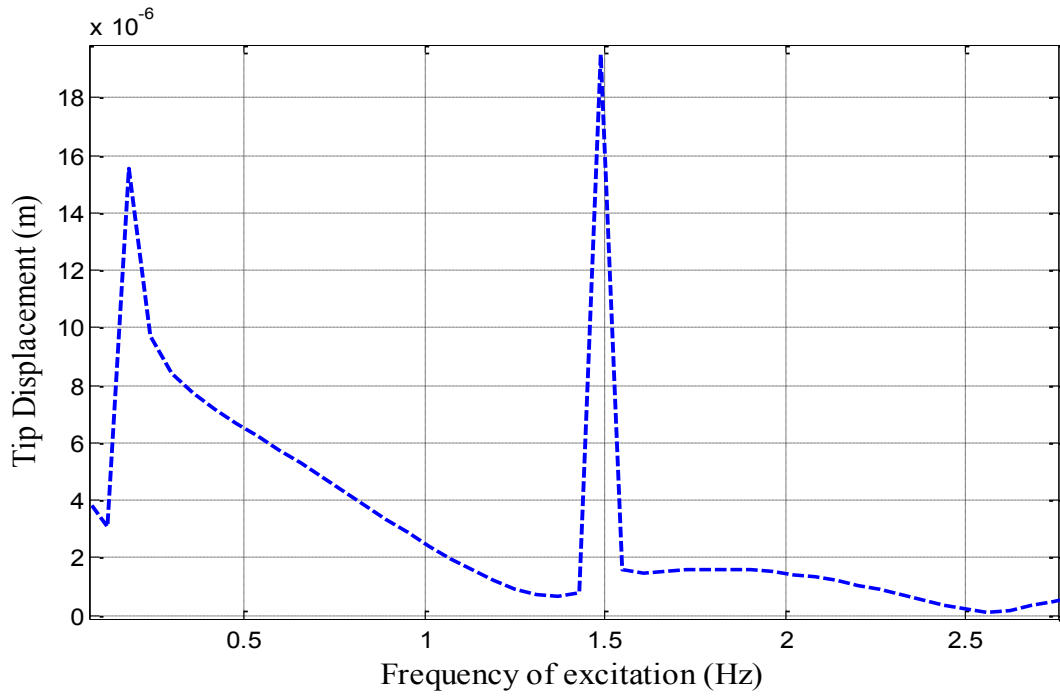
Figure 5.25: Tip deflection response of microcantilever 1 mm width X 7.5 mm length
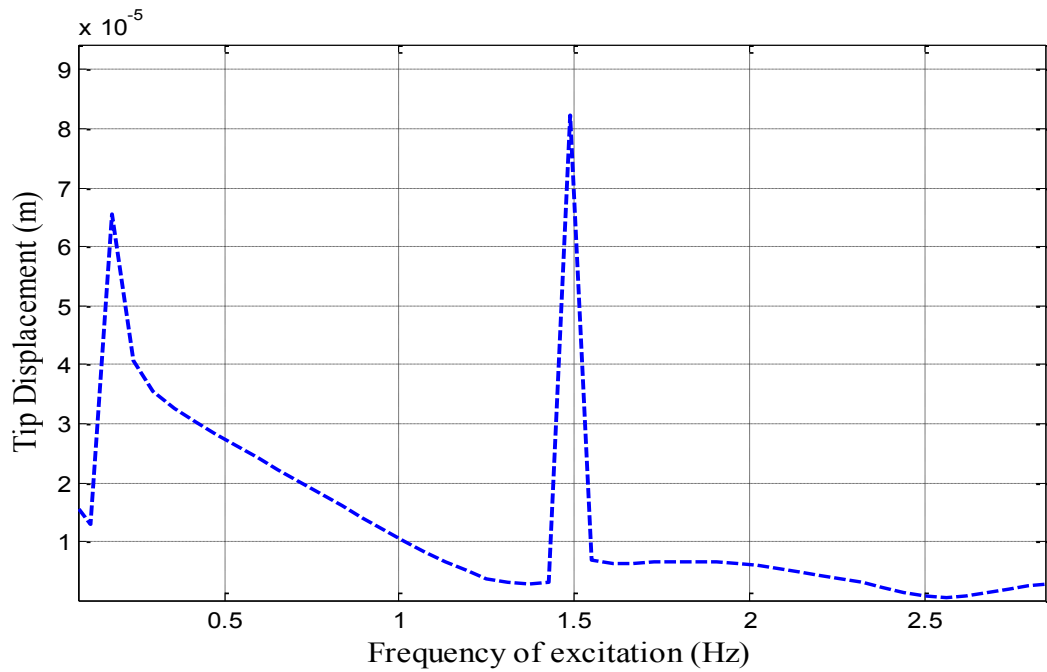
Figure 5.26: Tip deflection response of microcantilever 1 mm width X 10 mm length

Figure 5.27 - Figure 5.30 show frequency response of microcantilever with width 2 mm.

Similar trend can be observed as deflection amplitudes are found to be higher with longer beams.
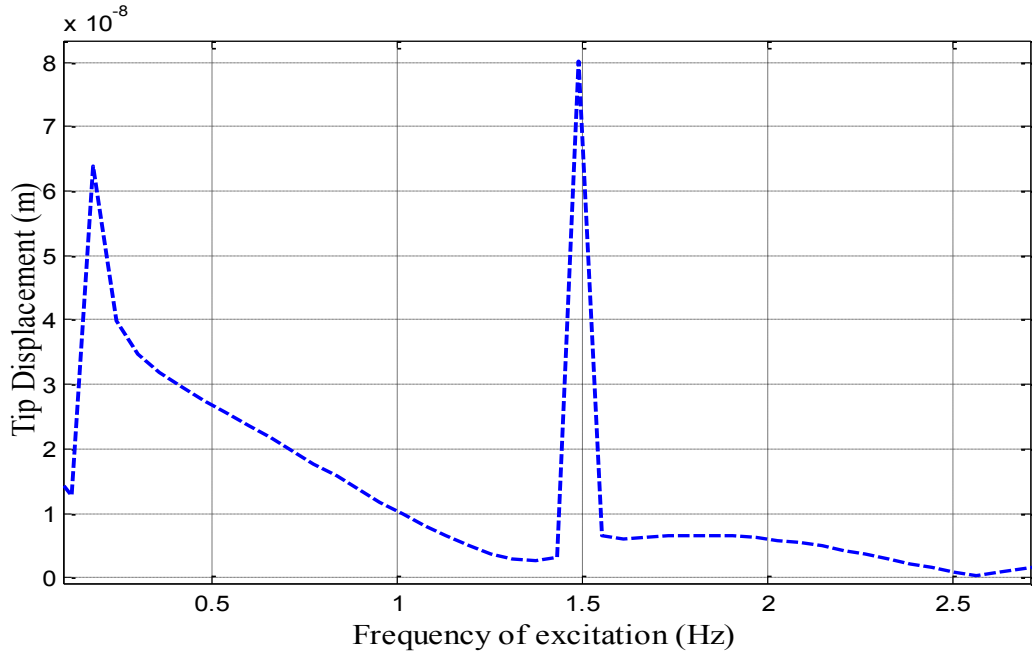
Figure 5.27: Tip deflection response of microcantilever 2 mm width X 2.5 mm length
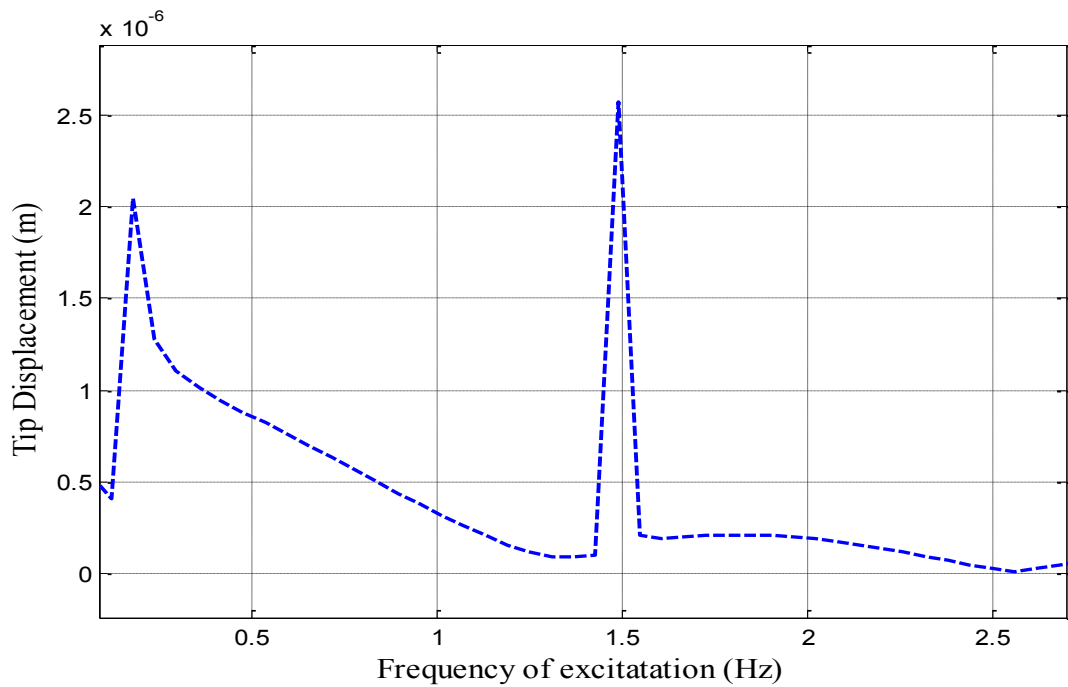
Figure 5.28: Tip deflection response of microcantilever 2 mm width X 5 mm length
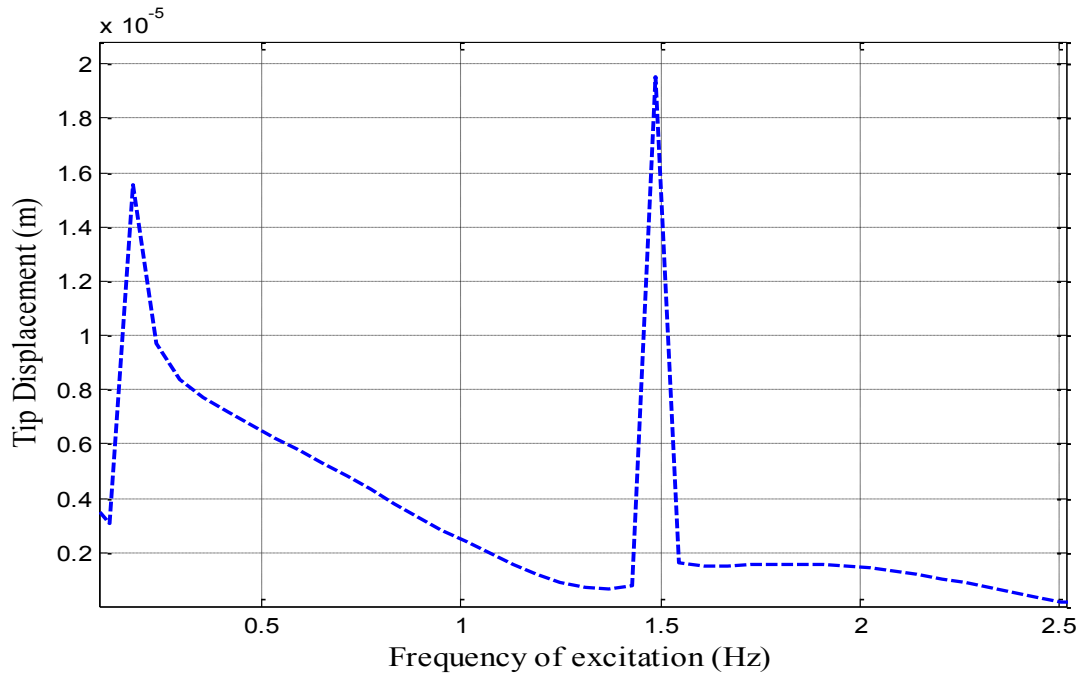
Figure 5.29: Tip deflection response of microcantilever 2 mm X 7.5 mm length
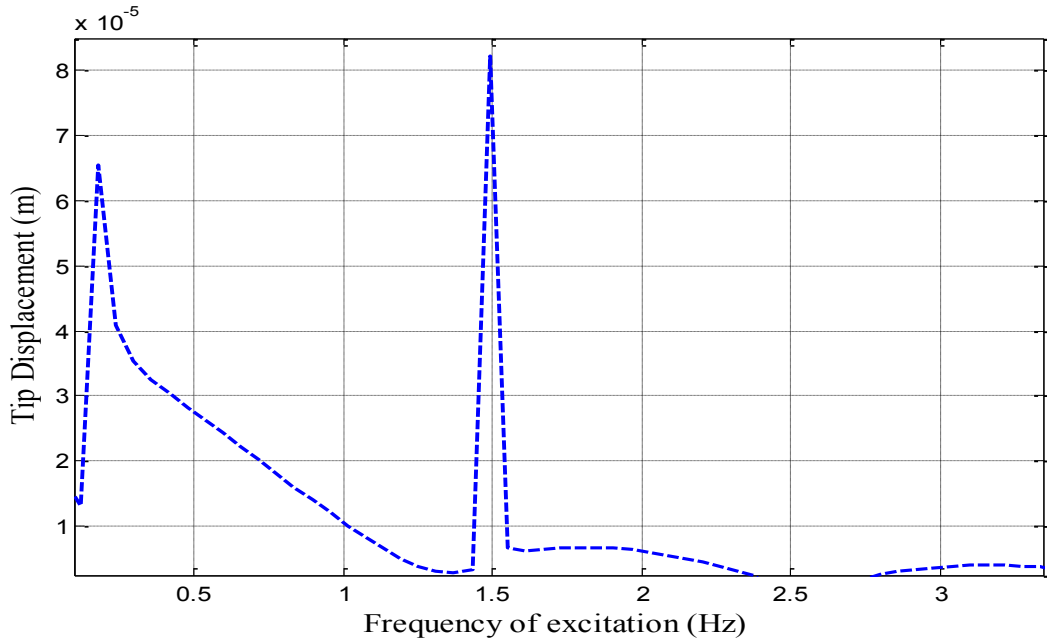
Figure 5.30: Tip deflection response of microcantilever 2 mm width X 10 mm length

Figure 5.31 - Figure 5.34 show frequency response of cantilevers having width 4 mm. Smallest amplitudes are observed with smaller lengths while amplitudes increase for longer beams.
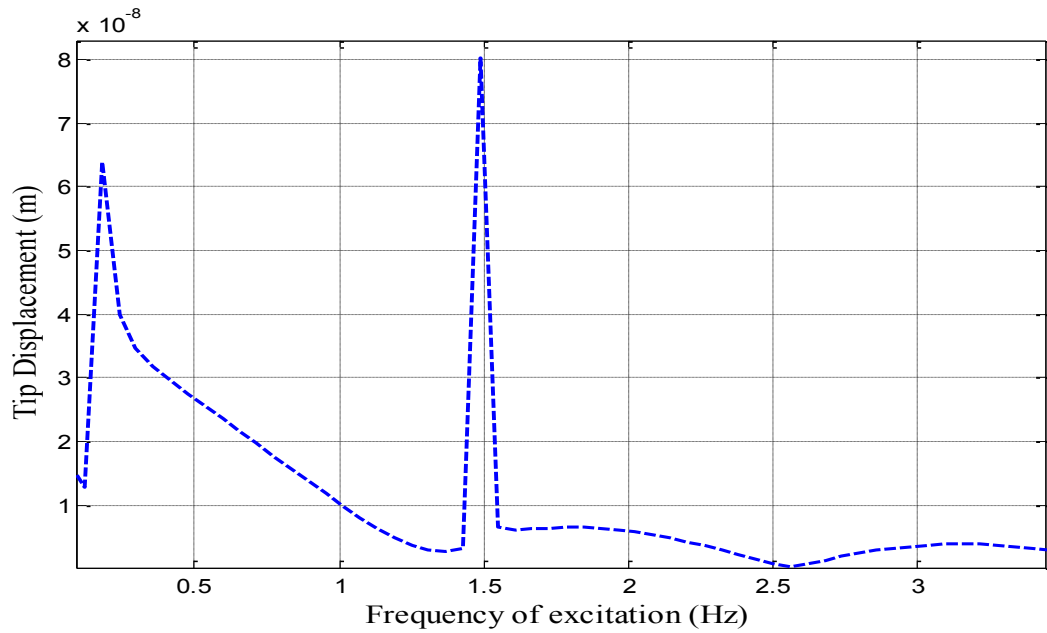
Figure 5.31: Tip deflection response of microcantilever 4 mm width X 2.5 mm length
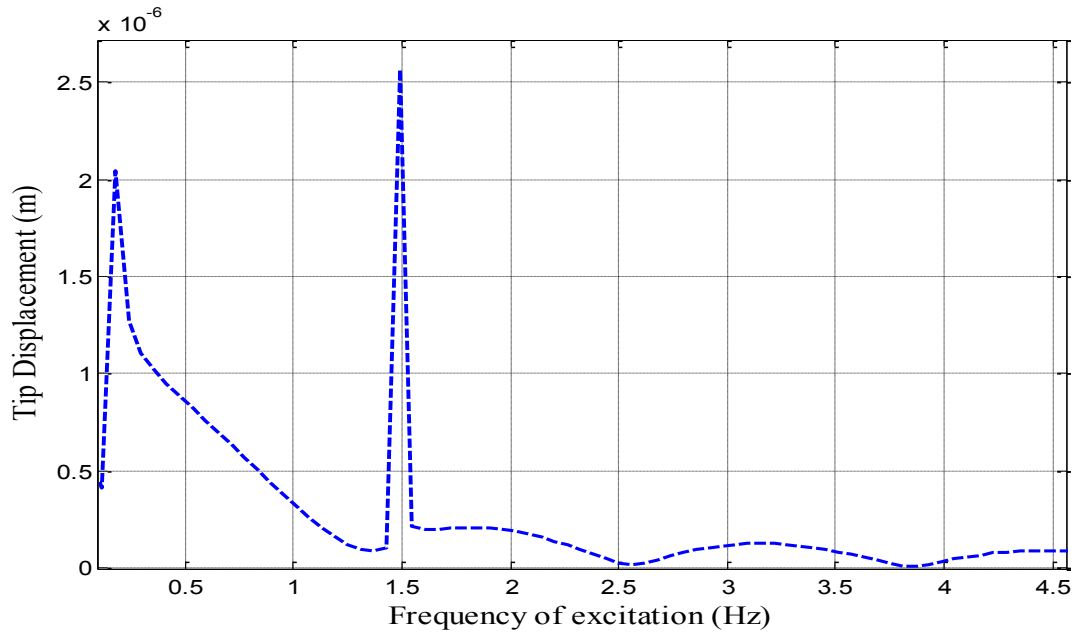
Figure 5.32: Tip deflection response of microcantilever 4 mm width X 5 mm length
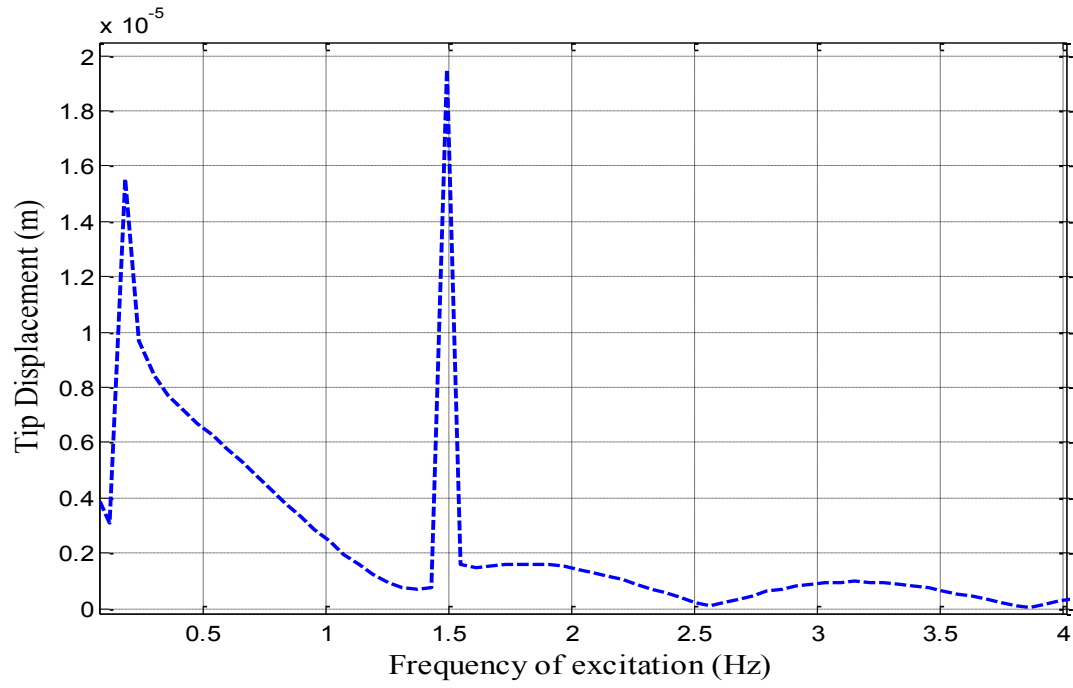
Figure 5.33: Tip deflection response of microcantilever 4 mm width X 7.5 length
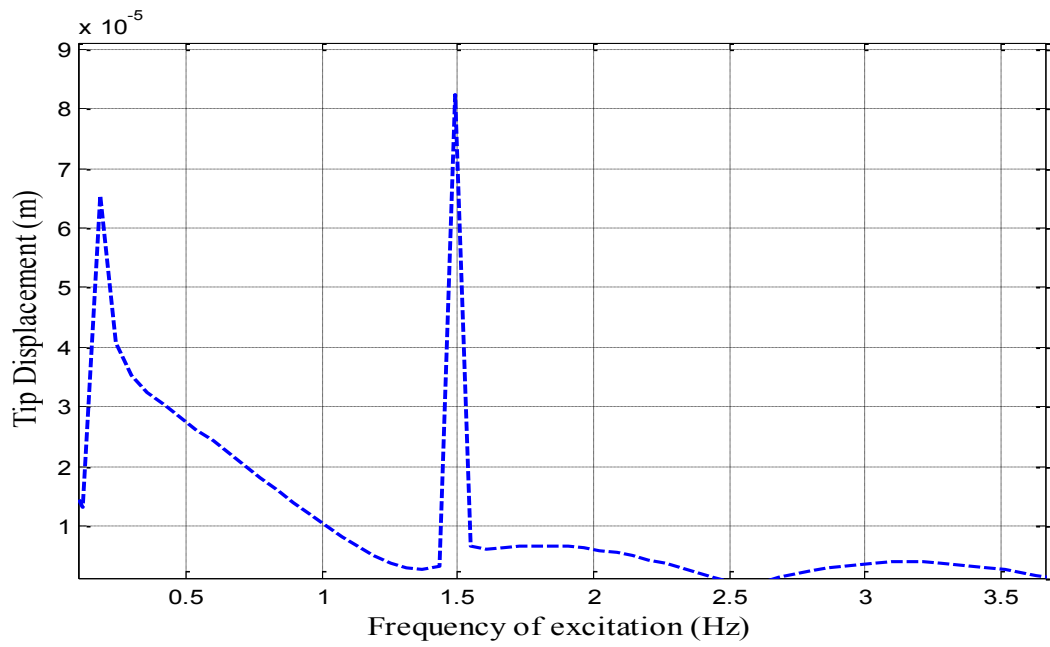
Figure 5.34: Tip deflection response of microcantilever 4 mm width X 10 mm length

As seen from above results, the increase in amplitudes is quite significant for lengths higher than 2.5 mm length.

Deflection amplitudes are tabulated for their respective lengths and widths.

Table 5.5: Deflection Amplitudes A_1 from Parametric study

Width (mm)	Length (mm)			
	2.5	5	7.5	10
	Amplitude A_1 (micron)			
0.5	0.1211	3.877	15.51	65.39
1	0.1037	2.047	15.55	65.51
2	0.06397	2.047	15.55	65.51
4	0.06397	2.047	15.55	65.51

Table 5.6: Deflection Amplitudes A_2 from Parametric study

Width (mm)	Length (mm)			
	2.5	5	7.5	10
	Amplitude A_2 (micron)			
0.5	0.1989	6.365	19.38	81.74
1	0.1376	2.57	19.52	82.32
2	0.0803	2.57	19.52	82.32
4	0.0803	2.57	19.52	82.32

All above results are plotted against respective lengths and widths and presented below.

Two deflection amplitudes are plotted seperately against all the combinations of lengths and widths of microcantilever as shown in Figure 5.35- Figure 5.36.
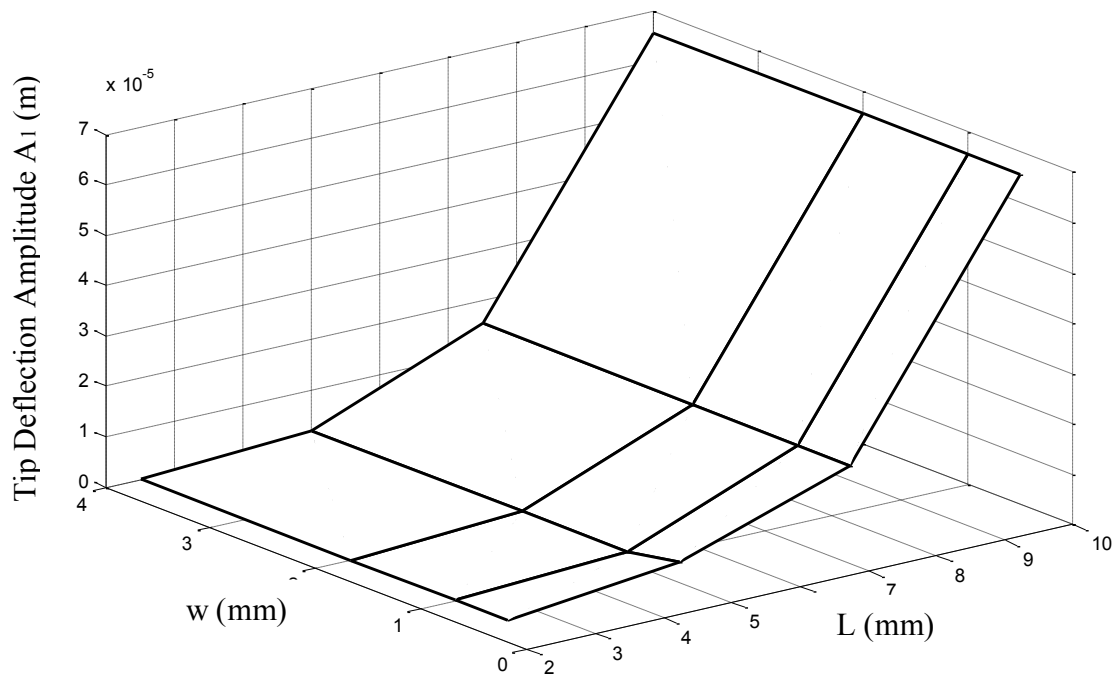
Figure 5.35: Deflection Amplitude A_1 plotted for various combinations of lengths and widths of microcantilever

Figure 5.35 shows tip deflection amplitudes A_1 for PVDF microcantilever plotted for 16 combinations of lengths and widths for a certain pressure loading and excitation frequency. It is observed that the amplitudes increase for higher lengths L of microcantielver for a certain width w. On the other hand, little variation is observed with the increase in widths of microcantilevers at a certain length.
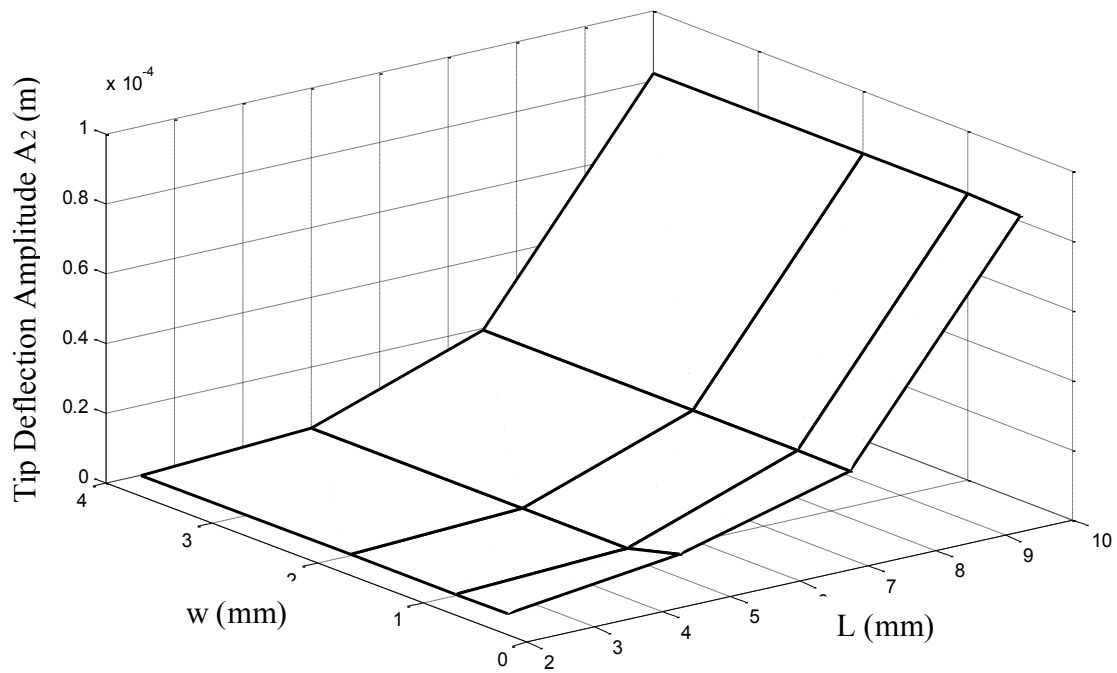
Figure 5.36: Deflection Amplitude A_2 plotted for various combinations of lengths and widths of microcantilever

Similarly, deflection amplitudes A_2 are plotted for the combinations of lengths and widths of microcantilever in Figure 5.36. Higher deflections can be observed with longer beams. Also, at a certain width, the variation of both amplitudes A_1 and A_2 against the aspect ratio is presented. Aspect ratio is defined as the ratio of length to width (L/w) of microcantilever.

Figure 5.37 shows variation of deflection amplitude A_1 with different aspect ratios for different widths of microcantilever. Amplitudes are plotted for each aspect ratio corresponding to each width. Higher amplitudes are observed for higher aspect ratios.
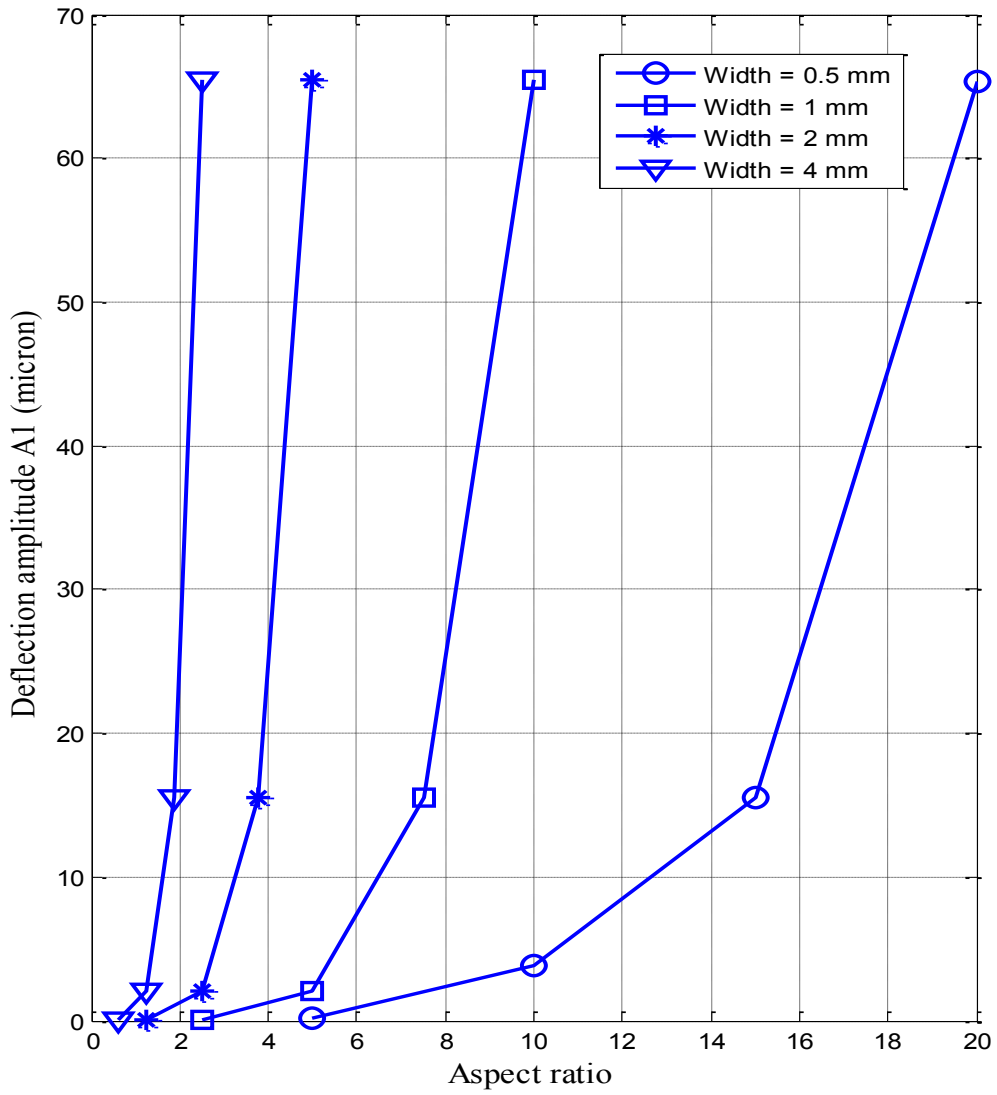
Figure 5.37: Deflection Amplitudes A_1 plotted for various aspect ratios for different widths
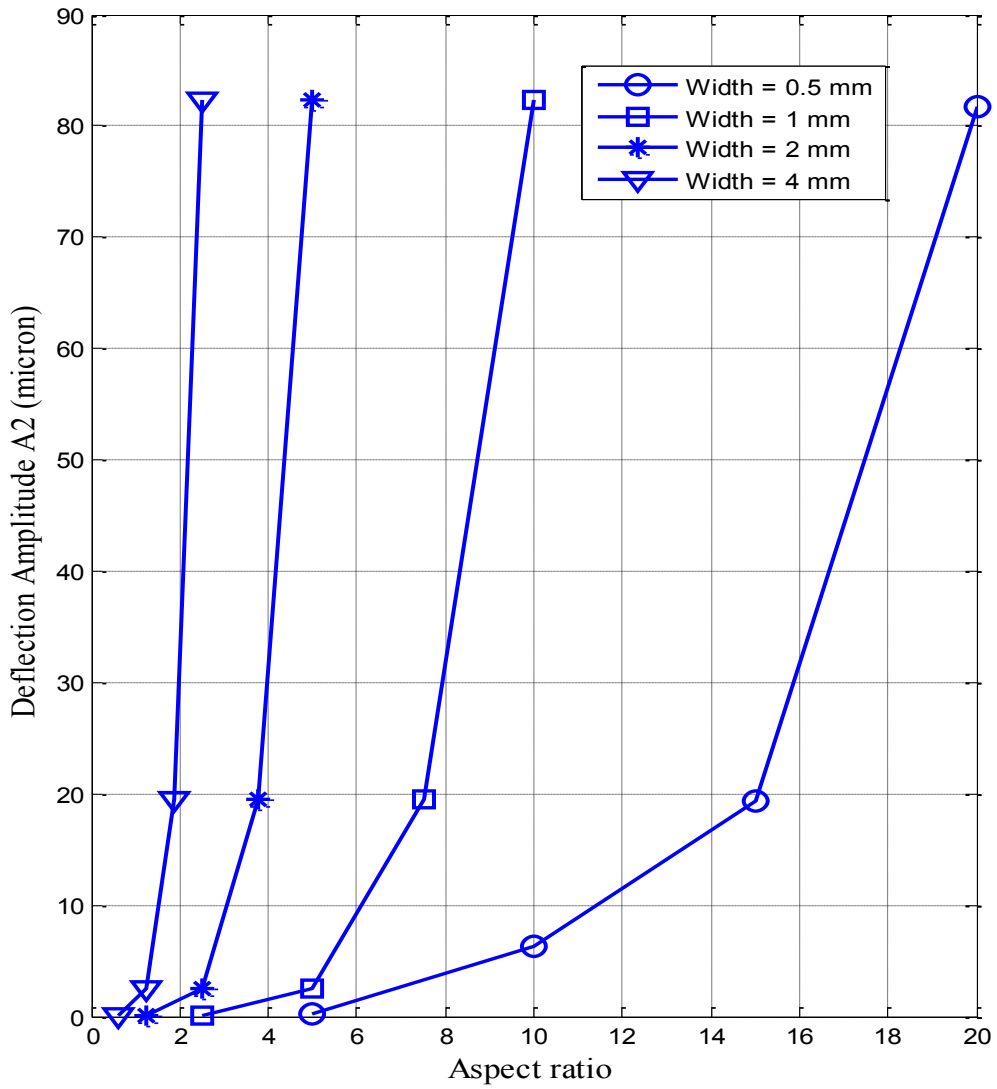
Figure 5.38: Deflection Amplitudes A₂ plotted for various aspect ratios for different widths

Similarly, Figure 5.38 shows variation of deflection amplitude A_2 with different aspect ratios corresponding to given widths.

5.4.2 Non Dimensionalized Amplitudes

Deflection amplitudes determined in parametric study are non-dimensionalized against corresponding fluid pressure loading and stiffness of the beam. Non dimensional parameter X has been obtained for each amplitude by dividing it by the ratio of force to respective stiffness. Non dimensional amplitudes of A_1 and A_2 are plotted against aspect ratio for a given width in Figure 5.39 - Figure 5.40.

Non-Dimensional parameter X is obtained as follows.

$$X_1 = \frac{A_1}{(F/k)}$$

$$X_2 = \frac{A_2}{(F/k)}$$

where A_1 and A_2 is the deflection amplitudes at ω_1 and ω_2.

F is the force due to fluid pressure loading.

k is the stiffness of the beam.

$$k = \frac{3EI}{L^3}$$

Figure 5.39 (a – d) and Figure 5.40 (a – d) show non-dimensionalized amplitudes X_1 and X_2 respectively for various aspect ratios at given widths. It provides data on the static and dynamic deflection amplitudes of microcantilevers of different aspect ratios vibrating under the action of two sets of fluid loading and excitation frequency.
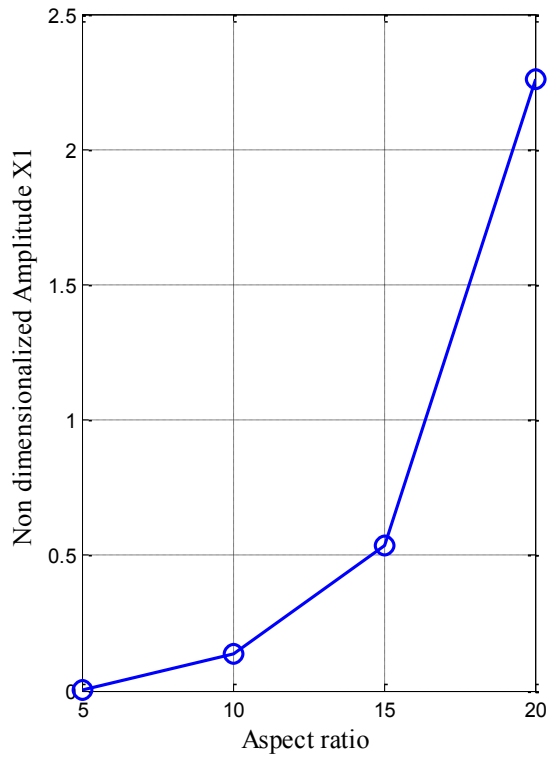
(a)
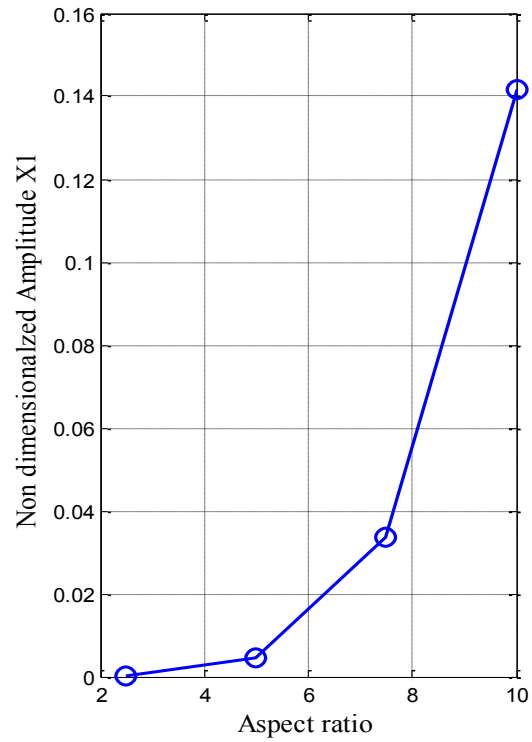
(b)
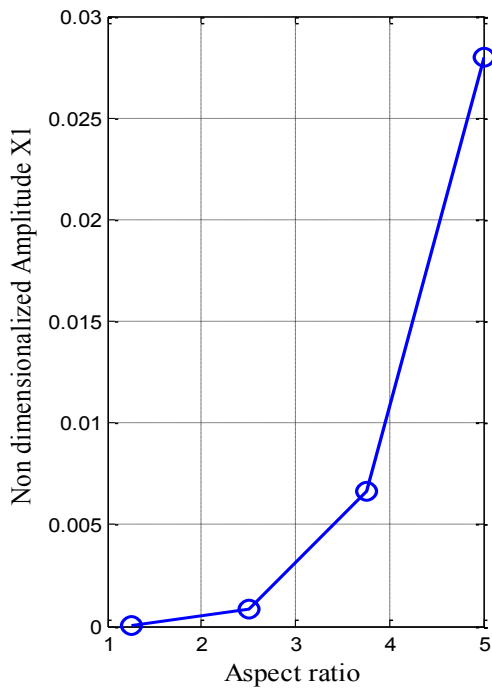
(c)
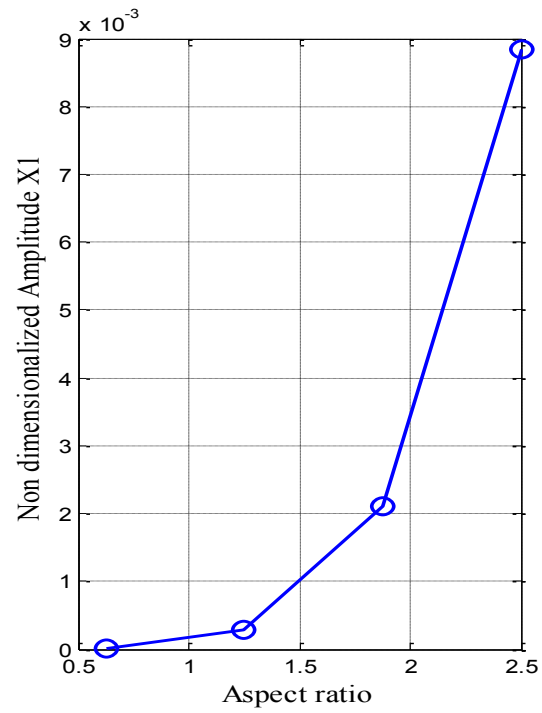
(d)

Figure 5.39: Non dimensional Amplitudes X_1 plotted for various aspect ratios (a)Width=0.5 mm (b)Width=1 mm (c)Width=2 mm (d)Width=4 mm
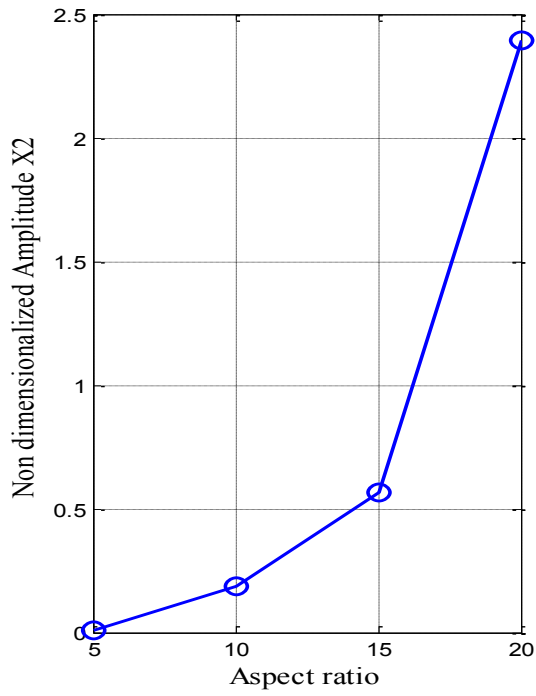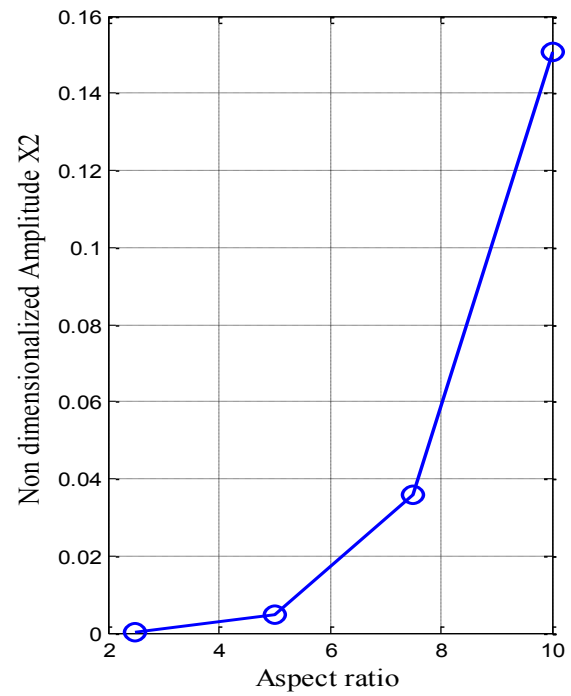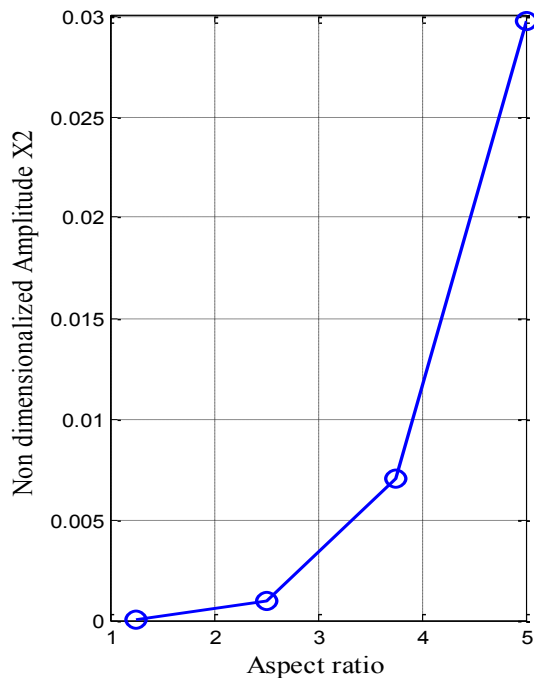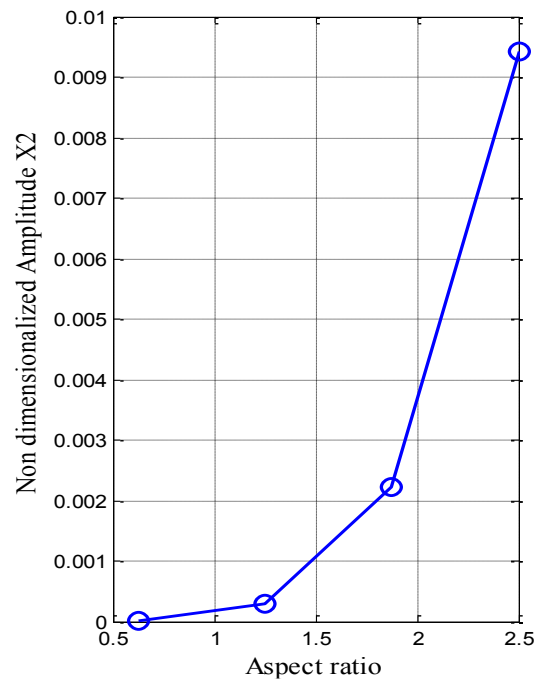
Figure 5.40: Non dimensional Amplitudes A_2 plotted for various aspect ratios (a)Width=0.5 mm (b)Width=1 mm (c)Width=2 mm (d)Width=4 mm

Chapter 6 Conclusion and future work

This chapter concludes the thesis by summarizing the preceding chapters. It also discusses applications and future work. The modeling of deflection response of a micro cantilever beam has been carried out for the fluid pressure loading and excitation frequency conditions in earlier experiments.

6.1   Conclusion

The main objective of this thesis is to present a numerical model of micro cantilever vibrating under the action of fluid loading. The dynamics of the micro cantilever is explored in order to understand its behavior under the action of fluid pressure loading. Following is the summary of preceding chapters.

1. Orthogonal polynomials have been created using Gram-Schmidt process and their use has been verified to find natural frequencies and mode shapes of cantilever beam and clamped plate.

2. A numerical model is presented using Mode Summation method to determine dynamic response of the micro cantilever using Euler Bernoulli equation of motion of beam.

3. Use of Simulink is presented to solve Euler Bernoulli equation of beam in time domain.

4. Deflection amplitudes of the beam are determined using Fast Fourier Transform and compared with those from earlier experiments.

5. Parametric study is performed to obtain dynamic deflections of microcantilevers of different lengths and widths. Deflections are plotted for different aspect ratios of

microcantilevers. Finally, deflection amplitudes are non-dimensionalized with respect to cantilever properties and fluid loading.

Following conclusions can be drawn from the present work.

1. The thesis describes the method to obtain deflection response of microcantilevers under the action of fluid loading. Fluid pressure loading is one of the parameters which affect the motion of flexible structures in fluid structure interaction system. It is a complicated process to obtain pressure loading in a numerical way for a particular dynamic system. The numerical method presented in this thesis serves as a start to the problems involving flexible systems encountering different types of fluid pressure loadings. The deflection amplitudes of PVDF microcantilever obtained from the numerical method presented in this work are compared with those from earlier experiment and they are found in agreement with each other.

2. The results from parametric study reveal that, the deflection amplitudes with longer microcantilever are higher as compared to those with shorter ones. On the other hand, the deflection amplitudes are slightly reduced for the wider microcantilevers than those with shorter widths.

6.2 Recommendations for future work

The numerical model offeres flexibility in determining the response of micro cantilever with considering added mass and added damping of fluid. The added mass calculated using one of the theories can be implemented in the matrix form of the equation and the equation can be solved to obtain deflection response using new mass.

$$[M + M_a]\{\ddot{\quad}\quad\dot{\quad}\quad\quad I\} = [P]$$

The model can be extended to explore dynamics of plate. The characteristic orthogonal polynomials generated in Chapter 3 can be used to obtain deflection response of plates under the action of fluid flow using Mode Summation method. The equation of motion of plate can be modeled in a similar way and solved using Simulink.

Fluid Pressure loading acting on a flexible structure is a crucial parameter for various systems while calculating its dynamic response. The kind of loading changes from one system to another. In the case of certain dynamic systems such as micropumps, the structural deformation may change the boundary conditions of the fluid. This change in fluid pressure is not considered in the present work. These changes can be determined with the help of modeling fluid equations such as Navier-Stokes equation. This equation has to be solved alongwith structural equation in order to obtain changes in fluid pressure in the vicinity of the structure.

REFERENCES

1   Vashist S. K., "A Review of microcantilevers for sensing applications", Journal of Nanotechnology,Vol.3, 2007.

2   Vidic. A., Then D., Ziegler C., "A new cantilever system for gas and liquid sensing.Ultramicroscopy", Vol.97,pp. 407-416, 2002.

3   Thundat T., Hansen K.M., " Microcantilever Biosensors", Methods,Vol.37, pp. 57-64, 2005.

4   Zhang J., Dai C., Su X., O'shea S.J., "Determination of Liquid density with a low frequency mechanical sensor based on Quartz tuning fork", Sens.Actuators B84, pp. 123-128, 2002.

5   Laser D.J., Santiago J.G., "A Review of Micropumps", Journal of Micromechanics and Microengineering,Vol.14, pp.R35-R64, 2004.

6   Olsson A., "Valveless Diffuser Micro-Pumps", Phd Dissertation, Royal Institute of Technology, Stockholm, 1998.

7   Song G., Fan B., Hussain F., "Simulation of piezoelectrically actuated valveless micropump", Journal of Smart Materials and Structures, Vol.14, pp.400-405, 2005.

8   Yadykin Y., Tenetov V., Levin D., "The added mass of a flexible plate oscillating in a fluid", Journal of Fluids and Structures, Vol. 17, pp.115-123, 2003.

9   Ergin A., Ugurlu B., "Linear vibration analysis of cantilevered plates partially submerged in fluids", Journal of Fluids and Structures, Vol. 17, pp.927-939, 2003.

10   Rezazadeh G., Fathalilou M., Shabani R.,"Dynamic characteristics and forced response of an electrostatically-actuated microbeam subjected fluid loading", Journal of Microsystems Technology, vol.15, pp.1355-1363, 2007.

11   Bhat R.B., "Natural frequencies of rectangular plates using characteristic polynomials in Rayleigh-Ritz method", Journal of Sound and Vibration, Vol.102, No.4, pp.493-499, 1985.

12   Cheung Y.K., Chakrabarti S., "Free vibration of thick, layered rectangular plates by a finite layer method", Journal of Sound and Vibration, Vol.21, No.3, pp.277-284, 1972.

13   Lucey A.D., Carpenter P.W., "The Hydrostatic stability of three-dimensional disturbances of finite compliant wall", Journal of Sound and Vibration, Vol.165, No. 3, pp.527-552. 1992.

14   Chen H.L., Wu J.H., Liu A.Q., "Exact solutions for free vibration analysis of Rectangular plates using Bessel functions", Journal of Applied Mechanics, Vol.74, pp.1247-1251, 2007.

15   Bouchaud J., Dixon R., "MEMS for Automotive applications: Prospects and strategic considerations", 11th International Forum on Advanced MicroSystems for Automotive Applications, 2007.

16   Wang X.Q., So R.M.C., Liu Y., "Flow-induced vibration of an Euler-Bernoulli beam", Journal of Sound and Vibration, Vol.243, pp.241-268, 2001.

17   Singuresu S. Rao., Vibration of Continuous Systems, Publisher: Wiley, Edition:2007

18   Yang H., Furlong C., "Analysis and Characterization of high-resolution MEMS pressure sensors", Proceedings of the 11th International Congress and Exposition, 2008.

19   MD Hossain S., "Microfluidic-Microstructure interaction study under oscillating flows: Design, modeling, testing and verifications", Master's thesis, Concordia University, 2010.

20   Sinha J.K., Singh S., Rao R., "Added Mass and damping of submerged perforated plates", Journal of Sound and Vibration, Vol.260, pp.549-564, 2002.

21   Fu Y., Price W.G., "Interactions between a partially or totally immersed vibrating cantilever plate and the surrounding fluid", Journal of Sound and Vibration, Vol.118, No.3, pp. 495-513.

22   Evensen D.A., "Nonlinear vibrations of beam with various boundary conditions", AIAA journal, Vol.6, No. 2, pp.370-372, 1968.

23   Oden P.I., Chen G.Y., Steele R.A., Warmack R.J. & Thundat T., "Viscous drag measurements utilizing microfabricated cantilevers", Applied Physics Letters, Vol.68, No.26, pp.3814-3816, 1996.

24   http://monet.physik.unibas.ch/nose/

25   http://www.ornl.gov/info/ornlreview/rev29-12/text/instru.htm

26   Barnes J.R., Stephenson R.J., Welland M.E., Gerber C. & Gimzewski J.K. "Photothermal spectroscopy with femtojoule sensitivity using a micromechanical device", Nature, Vol.372, pp.79-81, 1994.

27   Ji H.F., Thundat T., Dabestani R., Brown G.M., Britt P.F. & Bonnesen P.V., "Ultrasensitive detection of CrO42- using a microcantilever sensor. Analytical Chemistry", Vol.73, pp.1572-1576, 2001.

28   Wang Y.H., Hsueh T.H., Ma R.H., Lee C.Y., Fu L.M., Chou P.C., Tsai,T.H., "A microcantilever based gas flow sensor for flow rate and direction detection", DTIP of MEMS & MOEMS. 2008.

29   Houston B.H., Martin M.J., Fathy H.K., "Dynamic simulation of Atomic Force Microscope cantilevers oscillating in liquid", Journal of Applied Physics. Vol.104, 2008.

30   Pan F., Kubby J., Chen J., "Numerical simulation of fluid-structure interaction in a MEMS diaphragm drop ejector", Journal of Micromechanics and Microengineering, Vol.12, pp.70-76, 2002.

31   Woodhouse J., "Linear damping models for Structural vibration. Journal of Sound and Vibration", Vol.215, No.3, pp.547-569, 1998.

32   Vibration : Fundamentals and Practice by Clarence W.de Silva, Publisher: CRC/Taylor and Francis, Edition:2007

33   Kim B.S., Pettigrew M.J., Tromp J.H., "Vibration damping of heat exchanger tubes in liquids: Effects of support parameters", Journal of Fluids and Structures, Vol.2, pp.593-614, 1988.

34   Chon, J. W. M., Mulvaney P., and Sader, J. E., "Experimental validation of theoretical models for the frequency response of atomic force microscope cantilever beams immersed in fluids", Journal of Applied Physics, Vol. 87, No.8, pp. 3978-3988, 2000.

35   Chou, C. C., Lee, C. W. and Yang, M. H., "Simulation of an Atomic Force Microscopy's Probe Considering Damping Effect", Proceedings excerpt, COMSOL users conference, Taipei, Taiwan, 2007.

36   Clark, M. T. and Paul, M. R., "The stochastic dynamics of rectangular and V-shaped atomic force microscope cantilevers in a viscous fluid and near a solid boundary", Journal of Applied Physics, Vol. 103, No.9, pp. 094910-1, 2008.

37   Cole, D. G. and Clark, R. L., "Fluid-structure interaction in atomic force microscope cantilever dynamics and thermal response", Journal of Applied Physics, Vol. 101, No.3, pp. 34303-1, 2007.

38   Green, C. P. and Sader, J. E., "Frequency response of cantilever beams immersed in viscous fluids near a solid surface with applications to the atomic force microscope", Journal of Applied Physics, Vol. 98, No.11, pp. 114913-1, 2005.

39   Elmer, F., Dreier, M., "Eigenfrequencies of a rectangular atomic force microscope cantilever in a medium", Journal of Applied Physics, Vol. 81, No.12, pp.7709-14, 1997.

40   Martin, M. J., Fathy, H. K. and Houston, B. H., "Dynamic simulation of atomic force microscope cantilevers oscillating in liquid", Journal of Applied Physics, Vol. 104, No.4, pp. 044316-1, 2008.

41   Papi, M., Arcovito, G., De Spirito, M., Vassalli, M. and Tiribilli, B., "Fluid viscosity determination by means of uncalibrated atomic force microscopy cantilevers", Applied Physics Letters, Vol. 88, No.19, pp. 194102-1, 2006.

42   Foundations of MEMS by Chang Liu, Publisher: Prentice Hall, edition: 2005.

43   Chow S.T., Liew K.M., Lam K.Y., "Transverse vibrations of symmetrically laminated rectangular composite plates", Composite Structures, Vol.20, pp.213-226, 1992.

44   Nair P.S., Rao M.S., "On Vibration of plates with varying stiffener length", Journal of Sound and Vibration, Vol.95, pp.19-30, 1984.

45   Leissa A.W., "The free vibration of Rectangular plates", Journal of Sound and Vibration, Vol. 31, pp.257-293, 1973.

46   Chakraverty S., Bhat R.B., Stiharu I., "Recent research on vibration of structures using characteristic orthogonal polynomials in Rayleigh-Ritz method", The Shock and Vibration Digest, Vol.31, No.3, pp.187-194, 1999.

47   Wu J.R., Liu W.H., "Vibration of Rectangular plates with edge constraints and intermediate stiffeners", Journal of Sound and Vibration, Vol.123, No.1, pp.103-113, 1988.

48   Packirisamy M., "Boundary Conditioning concept applied to the synthesis of Microsystems using Fuzzy Logic Approach", PhD Thesis, Concordia University, 2000.

49   Matlab & Simulink HELP guides 2010.

50   Koch M., Evans A.G.R., Brunnschweiller A., "Characterization of micromachined cantilever valves", Journal of Micromechanics and Microengineering, Vol. 7, pp.221-223, 1997.

51   Sader J.E. "Frequency response of cantilever beams immersed in viscous fluids with applications to the Atomic force microscope", Journal of Applied Physics, Vol. 84, No.1, pp.64-76, 1998.

52   Leo A., "Development of Dynamic Pressure sensor for high temperature applications", PhD Thesis, Concordia University, 2010.

53   Turner A.P.F., "Current Trends in Biosensor Research and Development", Sensors Actuators, Vol.17, pp.433-450, 1989.

54   Zhang W., Turner K., "Frequency dependent fluid damping of micro/nano flexural resonators: Experiment, model and analysis", Sensors and Actuators, 2006.